



doi:10.1016/j.gca.2003.12.008

Nd-, O-, and H-isotopic evidence for complex, closed-system fluid evolution of the peralkaline Ilímaussaq intrusion, South Greenland

MICHAEL MARKS,¹ TORSTEN VENNEMANN,² WOLFGANG SIEBEL,¹ and GREGOR MARKL^{1,*}¹Institut für Geowissenschaften, AB Mineralogie und Geodynamik, Eberhard-Karls-Universität, Wilhelmstraße 56, D-72074 Tübingen, Germany²Institut de Minéralogie et Géochimie, Université de Lausanne, UNIL-FSH2, CH-1015 Lausanne, Switzerland

(Received May 13, 2003; accepted in revised form December 8, 2003)

Abstract—Relatively homogeneous oxygen isotope compositions of amphibole, clinopyroxene, and olivine separates (+5.2 to +5.7‰ relative to VSMOW) and neodymium isotope compositions ($\epsilon_{\text{Nd}(T)} = -0.9$ to -1.8 for primary magmatic minerals and $\epsilon_{\text{Nd}(T)} = -0.1$ and -0.5 for mineral separates from late-stage pegmatites and hydrothermal veins) from the alkaline to agpaitic Ilímaussaq intrusion, South Greenland, indicate a closed system evolution of this igneous complex and support a mantle derivation of the magma.

In contrast to the homogeneous oxygen and neodymium isotopic data, δD values for hand-picked amphibole separates vary between -92 and -232 ‰ and are among the most deuterium-depleted values known from igneous amphiboles. The calculated fluid phase coexisting with these amphiboles has a homogeneous oxygen isotopic composition within the normal range of magmatic waters, but extremely heterogeneous and low D/H ratios, implying a decoupling of the oxygen- and hydrogen isotope systems.

Of the several possibilities that can account for such unusually low δD values in amphiboles (e.g., late-stage hydrothermal exchange with meteoric water, extensive magmatic degassing, contamination with organic matter, and/or effects of Fe-content and pressure on amphibole-water fractionation) the most likely explanation for the range in δD values is that the amphiboles have been influenced by secondary interaction and reequilibration with D-depleted fluids obtained through late-magmatic oxidation of internally generated CH_4 and/or H_2 . This interpretation is consistent with the known occurrence of abundant magmatic CH_4 in the Ilímaussaq rocks and with previous studies on the isotopic compositions of the rocks and fluids. *Copyright © 2004 Elsevier Ltd*

1. INTRODUCTION

On the basis of stable and radiogenic isotope studies, the petrogenesis of undersaturated and oversaturated peralkaline igneous rocks is believed to be different: alkaline silica-undersaturated intrusive rocks are commonly explained by fractional crystallization of mildly alkalic or transitional basalts with negligible minor or without crustal contamination (e.g., Larsen and Sørensen, 1987; Perry et al., 1987; Kramm and Kogarko, 1994; Schmitt et al., 2000). For example, the peralkaline to agpaitic silica-undersaturated rocks of the intrusive complexes of Khibina and Lovozero (Russia) are regarded as residues formed in the upper mantle by fractional crystallization from nephelinites, basanites or nepheline benmoreites. They have isotopic compositions similar to those of a depleted melt source, but there is no sign of any assimilation of crustal melts in these rocks (Kramm and Kogarko, 1994). In contrast, alkaline to peralkaline silica-oversaturated intrusive rocks typically show signs of contamination with crustal material during emplacement (e.g., Davies and Macdonald, 1987; Heaman and Machado, 1992; Harris, 1995; Mingram et al., 2000; Schmitt et al., 2000; Späth et al., 2001; Marks et al., 2003). For example, studies on silica-undersaturated, oversaturated, and mixed complexes of the Damaraland, Namibia (Harris et al., 1990, 1999; Harris, 1995; Mingram et al., 2000; Schmitt et al., 2000) and from the Gardar province of South Greenland (e.g., Marks et al., 2003) support the assumption of Foland et al. (1993) that

alkaline silica-oversaturated magmas evolved from undersaturated magma via crustal contamination, or that they are products of crustal anatexis.

The Gardar Igneous Province in South Greenland is characterized by the occurrence of a number of classic alkaline igneous complexes that are exceptionally well preserved and, as a result, have been examined in detail for their mineralogical and geochemical compositions (e.g., Ferguson, 1964; Emeleus and Upton, 1976; Larsen, 1976; Upton and Emeleus, 1987; Bailey et al., 2001; Markl et al., 2001a; Sørensen, 2001; Upton et al., 2003). However, despite the good preservation, detailed studies of the stable and radiogenic isotopic compositions of these rocks to evaluate the influence and extent of crustal contamination have been relatively limited (e.g., Blaxland et al., 1976; Sheppard, 1986a; Stevenson et al., 1997; Marks et al., 2003). Recent detailed mineralogical and isotopic studies on the silica-saturated to oversaturated Puklen complex in the western part of the Gardar Province indicated the importance of a crustal component for the genesis of this complex (Marks et al., 2003). Nd isotope compositions for primary minerals were found to be highly variable, indicating that assimilation of crustal rocks occurred to different extents. Furthermore, O-isotopic compositions of different minerals from the same sample indicate a multi-source genesis and a major late-stage influx and circulation of an externally derived fluid phase in the Puklen magma chamber.

Published works on the Ilímaussaq intrusion are more difficult to interpret, as these studies are at odds with each other and with the petrologic information. For example, the Sr-, O-, and H-isotope data summarized in Sheppard (1986a; also given in

* Author to whom correspondence should be addressed (markl@uni-tuebingen.de).

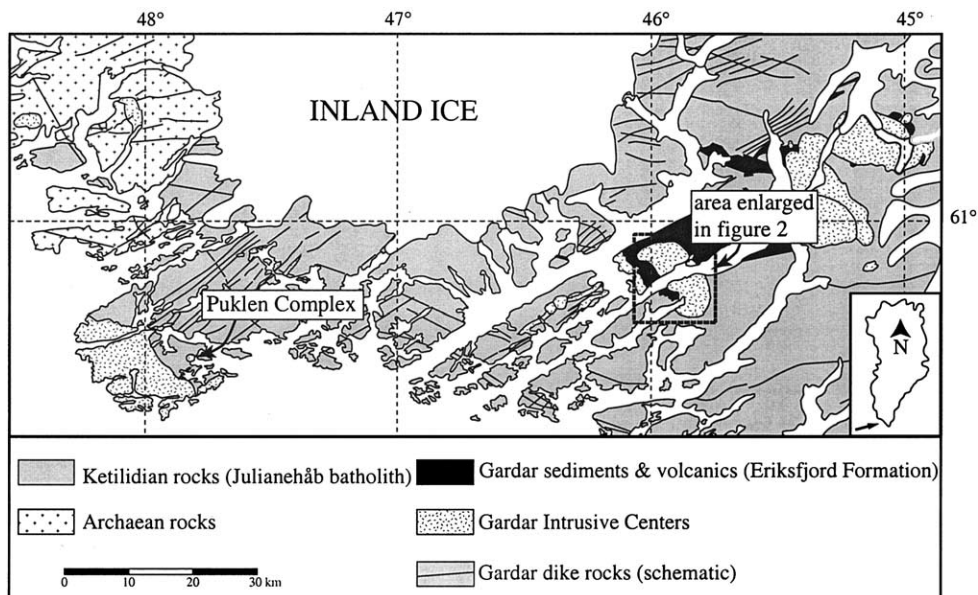


Fig. 1. Geological sketch map of the alkaline Gardar Province, South Greenland (modified after Escher and Watt, 1976). Note the outcrop of Archaean rocks in the northwestern part of the province. The Ilímaussaq intrusion is demonstrated in the dashed frame and illustrated enlarged in Figure 2. The Puklen complex is a location referred to in the text.

Konnerup-Madsen, 1980) have been interpreted to indicate significant crustal contamination for the complex as a whole. In particular, the extremely low D/H ratios of the hydrous silicates of the Ilímaussaq peralkaline igneous rocks (Sheppard, 1986a) have been taken to indicate a contaminant rich in organic matter. This is in contrast to the whole rock Nd-isotope data presented by Stevenson et al. (1997) suggesting limited crustal contamination only in the marginal facies of the complex and in the alkali granite, which would be in accordance with the mineralogy and petrology of this complex (e.g., Larsen, 1976; Bailey et al., 2001; Markl et al., 2001a; Marks and Markl, 2001; Sørensen, 2001; Upton et al., 2003). Another complexity arises, as the Ilímaussaq intrusion is a classical example of a peralkaline to agpaite igneous complex, where molecular hydrogen, methane and other hydrocarbons dominate the magmatic fluid phase. Such highly reduced conditions of crystallization have been recognized to be of importance in many alkaline, peralkaline and agpaite igneous rocks (e.g., Petersilie and Sørensen, 1970; Kogarko et al., 1987; Nivin et al., 1995; Salvi and Williams-Jones, 1997; Potter et al., 1998), but there is a matter of controversy, with models varying between mantle-derived, late-stage magmatic or of extraneous origin (e.g., Konnerup-Madsen and Rose-Hansen, 1984; Salvi and Williams-Jones, 1997; Potter et al., 1998, Konnerup-Madsen, 2001). Measurements of the C- and H-isotopic compositions of methane-rich fluid inclusions in the Ilímaussaq rocks are, however, consistent with a magmatic origin (Konnerup-Madsen and Rose-Hansen, 1984; Konnerup-Madsen, 2001), and not with an organic source as in the model of Sheppard (1986a).

In an attempt to resolve some of the controversial isotopic data for the Ilímaussaq intrusion and to determine whether or not a relationship exists between the late-stage methane-rich fluids and the low D/H ratios of the amphiboles, the present Nd-, O- and H-isotopic study of mineral separates of the major

rock types (in contrast to whole rocks used in the previous studies), and of late-stage hydrothermal veins of the Ilímaussaq intrusion has been initiated. In addition, oxygen and hydrogen isotope data have the potential to characterize the late-stage fluid evolution and to decipher the processes taking place during late- to postmagmatic cooling (e.g., Taylor, 1986; Taylor and Sheppard, 1986; Agemar et al., 1999; Harris and Ashwal, 2002; Dallai et al., 2003), because the hydrogen isotopic compositions of hydrous minerals are particularly sensitive indicators of the isotopic composition of the last fluid with which they equilibrated due to the relatively small amounts of hydrogen relative to the interacting fluid, they contain except at very small fluid-rock ratios (e.g., Gregory and Criss, 1986). As late-stage fluids at the Ilímaussaq intrusion produced economically interesting enrichments of U, Th, REE and Be (e.g., Sørensen et al., 1974; Engell et al., 1971), understanding these processes is of general interest as well.

2. GEOLOGICAL SETTING AND PREVIOUS STUDIES

The Gardar Province of South Greenland (Fig. 1) represents a Mid-Proterozoic (1.1–1.3 Ga) failed continental rift structure (Upton and Emeleus, 1987; Upton et al., 2003). The Early-Proterozoic (1.80–1.85 Ga) basement rocks (I-type calc-alkaline plutonic rocks; Julianehåb batholith; e.g., Kalsbeek and Taylor, 1985; Garde et al., 2002) are in places overlain by a sequence of basalts and sandstones (Eriksfjord Formation; Poulsen, 1964). A large number of dike rocks and twelve major alkaline to peralkaline igneous complexes intruded the basement at shallow crustal levels (<5 km) and they are believed to have had surface expressions (Emeleus and Upton, 1976; Upton et al., 2003). Among these complexes, principally two different subgroups can be distinguished: those evolving from silica-saturated syenites to alkali granites, following a silica-

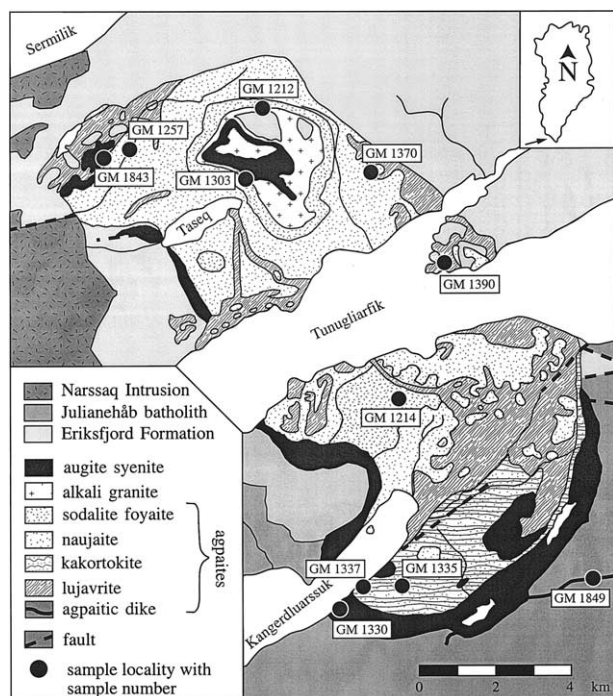


Fig. 2. Geological sketch map of the Ilímaussaq intrusion after Ferguson (1964), showing sample localities.

oversaturated trend, and those following a silica-undersaturated trend, evolving towards nepheline syenites.

The 1.16 Ga old Ilímaussaq complex (e.g., Blaxland et al., 1976; Waight et al., 2002) is the only intrusive complex of the Gardar province where both silica-undersaturated and silica-oversaturated rocks occur in significant quantities (Fig. 2). The formation of the complex involved three magma batches, which intruded successively to 3–4 km depth (1 kbar; Konnerup-Madsen and Rose-Hansen, 1984; Larsen and Sørensen, 1987). The earliest melt batch consists of augite syenite, which was later intruded by alkali granite. The third intrusive phase is represented by different varieties of agpaitic syenites that form the major part of the complex. They are grouped into roof cumulates (sodalite foyaite, naujaite), floor cumulates (kakortokite) and residual liquids (lujavrites). It is believed that all Ilímaussaq rocks were derived from one parental alkali basaltic magma that fractionated in a deep-seated magma chamber (Nielsen and Steinfelt, 1979; Larsen and Sørensen, 1987; Stevenson et al., 1997).

The Rb-Sr whole-rock study of Blaxland et al. (1976) points to a “primitive” mantle reservoir for the augite syenite, but a later introduction of radiogenic Sr into the agpaitic magma. The Sm-Nd whole-rock study of Stevenson et al. (1997) showed that all of the Ilímaussaq rocks could principally have been derived from the same mantle reservoir through fractional crystallization of a basaltic melt whilst assimilating granitic crust. However, extensive contamination took place only at the margins of the complex (Ferguson, 1964; Stevenson et al., 1997; Marks and Markl, 2001).

The petrology and mineral chemistry of the major rock-forming minerals in the various rock types was presented by Larsen (1976, 1977, 1981), Markl (2001a), Markl et al.

(2001a,b), and Marks and Markl (2001). The fractionation trend found in the Ilímaussaq complex is governed by low activities of water and SiO₂, which in turn are dependent on low oxygen fugacities in the parental melt. This results in highly reduced phase assemblages and in allowing the coexistence of two immiscible fluids (a methane-dominated gaseous and a highly saline aqueous fluid phase) during most of the crystallization history (Larsen, 1976; Konnerup-Madsen et al., 1979, 1988; Konnerup-Madsen and Rose-Hansen, 1984; Konnerup-Madsen, 2001; Markl et al., 2001a; Marks and Markl, 2001).

3. PETROGRAPHY AND MINERAL CHEMISTRY

3.1. Sample Description

From each of the major rock types of the complex, one representative sample was selected for mineral chemical, oxygen, hydrogen, and neodymium isotope analyses. Additional samples were selected from late-stage pegmatites, dikes and mineralized veins. The sample localities are shown on Figure 2. Detailed descriptions of the major rock types have been presented in many publications (e.g., Ferguson, 1964). Therefore, only brief descriptions of the investigated samples of this study are given with special focus on amphibole and aegirine textures, since most Nd, O, and H isotope analyses were performed on separates of these minerals. The mineral chemistry and petrology of most of the samples analyzed here have already been discussed in Markl (2001b), Markl et al. (2001a), and Marks and Markl (2001).

3.1.1. Augite Syenite (GM1330)

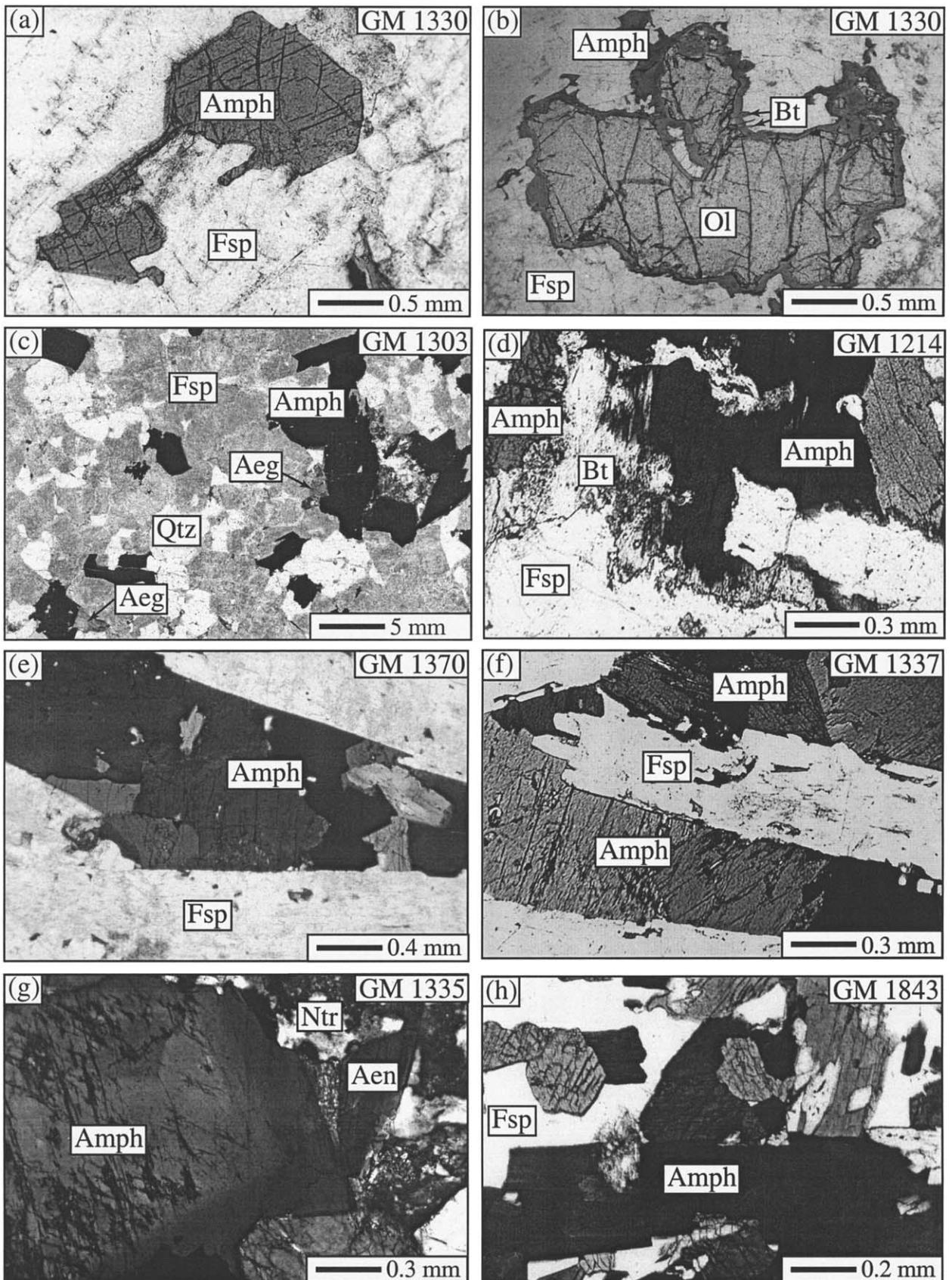
Early magmatic phases are alkali feldspar, apatite, baddeleyite, olivine, augite, Ti-magnetite, and less abundant amphibole (Fig. 3a). Nepheline occurs as an interstitial phase. Fine-grained biotite and amphibole form small rims around olivine, augite or Ti-magnetite and are believed to be of late-magmatic to hydrothermal origin (Fig. 3b). Magmatic and late-stage amphibole can be distinguished by their different grain size: magmatic amphibole can reach a size of up to 2 mm, whereas late-stage amphibole rims are less than a few hundreds of micrometers thick.

3.1.2. Alkali Granite (GM1303)

The sample is coarse-grained and equigranular. Euhedral amphibole, alkali feldspar, and zircon are early magmatic phases, abundant quartz occurs interstitially. In some places, late-stage aegirine aggregates overgrow early magmatic amphibole (Fig. 3c).

3.1.3. Agpaitic Syenites (GM1214, GM1370, GM1335, GM1337, GM1843)

Early magmatic phases in the medium- to coarse-grained nepheline syenites are alkali feldspar, nepheline, sodalite, amphibole, olivine and augite. The latter two occur only as rare relics in sample GM1214 (sodalite foyaite). Depending on the type of agpaitic syenite, interstitial phases are aegirine-augite, aenigmatite, fluorite, eudialyte, amphibole, sodalite and nepheline (Figs. 3d–h). Late-stage minerals are biotite, aegirine, and



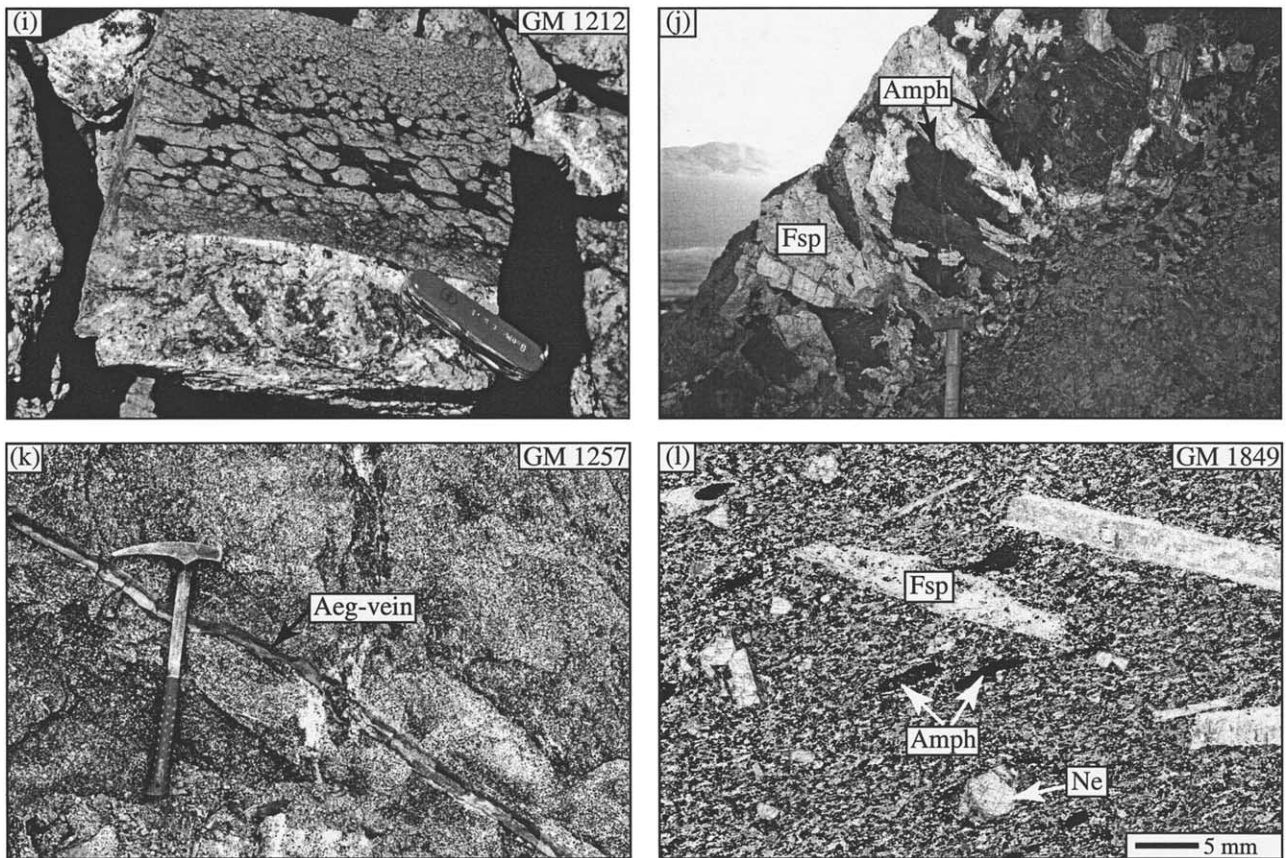


Fig. 3. Micro-textures and field relations observed for the different rock types. (a) Subhedral amphibole in a matrix of feldspar in augite syenite. (b) Fayalitic olivine rimmed by amphibole and biotite in augite syenite. (c) Subhedral amphibole in a matrix of feldspar and quartz in alkali granite. (d) Amphibole together with biotite in sodalite foyaite. (e) Interstitial amphibole in naujaite. (f) Interstitial amphibole in black kakortokite. (g) Euhedral and chemically zoned amphibole together with aenigmatite and natrolite in red kakortokite. (h) Euhedral amphibole in lujavrite. (i) Exsolved lujavrite consisting of a fine-grained black matrix, and gray, partly deformed ocelli. Pocketknife for scale. (j) Agpaitic pegmatite consisting of huge crystals of feldspar and amphibole. The latter is partly overgrown by aegirine coatings (not visible). The head of the hammer is ~12 cm in size. (k) Late-stage aegirine-albite-analcime vein intruding naujaite. Length of hammer is approximately 40 cm. (l) Porphyritic texture in an agpaitic dike rock in the vicinity of the Ilímaussaq intrusion. Abbreviations: aeg = aegirine, aen = aenigmatite, amph = amphibole, bt = biotite, fsp = feldspar, ne = nepheline, ntr = natrolite, ol = olivine, qtz = quartz.

analcime. One fine-grained agpaitic rock type (lujavrite, GM1843) shows fluidal textures. Early mineral phases in this sample are euhedral nepheline, eudialyte, and sodalite, which are enclosed in a fine-grained mixture of albite, microcline, and later generations of aegirine and arfvedsonite (for more details see e.g., Ferguson, 1964).

3.1.4. Agpaitic Dike Rock (GM1849)

Southeast of the Ilímaussaq intrusion, an agpaitic dike, several meters in thickness, is believed to be closely related to the Ilímaussaq rocks and can be traced for ~18 km. (Allaart, 1969; Larsen and Steinfeldt, 1974; Marks and Markl, 2003). Phenocrysts in the analyzed sample are olivine, augite, magnetite, alkali feldspar and nepheline (Fig. 3l). The groundmass consists of aegirine, aenigmatite, arfvedsonite, albite, microcline, nepheline, and sodalite (Marks and Markl, 2003). Similar dike rocks from other parts of the Ilímaussaq intrusion have been described by Rose-Hansen and Sørensen (2001).

3.1.5. Agpaitic Dike with Ocelli Textures (GM1212)

Some agpaitic dikes exhibit spectacular features of macroscopically visible liquid immiscibility. They can be found at several places distributed over the whole intrusion. These dikes are up to several hundreds of meters long, but less than a meter wide. They consist of a fine-grained black matrix and light grayish to greenish rounded and partly deformed ocelli (Fig. 3i). A detailed description and discussion of these rocks is given by Markl (2001b). The sample analyzed for this study consists of splits from the black and fine-grained matrix of sample GM1212, which is modally dominated by tiny euhedral amphibole.

3.1.6. Agpaitic Pegmatite (GM1390)

Sample GM 1390 is an agpaitic pegmatite (Fig. 3j). It consists of cm-to dm-sized K-feldspar and arfvedsonitic amphi-

Table 1. Representative microprobe analyses of amphiboles of the different rock types.^a

Sample rock type	GM1330 augite syenite ferropargasite		GM1303 alkali granite arfvedsonite		GM1214 sodalite foyaite arfvedsonite/ ferric- ferroxyböite		GM1370 naujaite arfvedsonite		GM1337 kakortokite (black) arfvedsonite/ ferric- ferroxyböite		GM1843 lujavrite arfvedsonite		GM1849 appaitic dike arfvedsonite	
	SiO ₂	40.82	39.13	49.22	49.88	46.68	48.27	49.07	50.74	48.13	47.32	50.76	50.74	48.79
TiO ₂	0.35	3.10	1.52	0.55	0.58	0.64	0.50	0.50	0.75	0.71	0.54	0.82	0.38	0.46
Al ₂ O ₃	9.11	10.76	0.29	0.21	3.05	1.83	2.18	0.91	2.68	3.20	0.65	0.70	2.30	2.33
ZnO	0.06	0.07	0.39	0.28	n.d.	n.d.	0.45	0.37	0.16	0.48	0.28	0.22	n.d.	n.d.
Li ₂ O	0.01	0.01	0.18	0.10	n.d.	n.d.	0.30	0.37	0.13	0.13	0.38	0.39	n.d.	n.d.
FeO	29.00	27.17	32.96	35.19	34.62	35.37	33.30	32.87	32.81	32.80	32.37	31.22	33.10	33.54
MnO	0.50	0.48	0.78	0.48	0.84	0.74	0.93	0.95	0.70	0.63	1.26	1.22	1.00	1.06
MgO	3.12	2.57	0.00	0.10	0.36	0.03	0.08	0.14	1.00	1.00	0.01	0.02	0.50	0.49
CaO	10.26	10.39	0.25	0.22	2.39	1.62	1.00	0.64	1.18	1.50	0.15	0.16	1.08	1.23
Na ₂ O	3.04	3.19	8.55	8.66	7.33	7.70	9.61	8.73	8.63	8.38	8.67	8.85	7.30	7.31
K ₂ O	1.69	1.63	1.46	1.17	1.95	1.86	2.02	2.90	2.14	1.92	3.00	3.08	2.71	2.54
ZrO ₂	0.32	0.38	0.14	0.11	0.20	0.01	0.07	0.04	0.20	0.65	1.12	1.55	0.04	0.02
Cl	0.06	0.13	0.03	0.03	0.00	0.00	0.00	0.00	0.00	0.01	0.02	0.01	0.00	0.00
F	1.04	0.33	3.29	1.37	0.79	0.56	0.00	0.00	0.07	0.03	0.00	0.00	0.04	0.03
Total	98.99	98.88	99.05	98.36	98.79	98.65	98.69	98.38	98.43	98.25	99.20	98.96	97.23	97.47
Formulae based on 16 cations and 23 oxygens														
Si	6.50	6.21	7.98	8.00	7.45	7.71	7.50	7.82	7.50	7.41	7.88	7.87	7.82	7.76
Al	1.71	2.01	0.06	0.04	0.57	0.34	0.39	0.16	0.49	0.59	0.12	0.13	0.43	0.44
Ti	0.04	0.37	0.18	0.07	0.07	0.08	0.06	0.06	0.09	0.08	0.06	0.10	0.05	0.06
Zn	0.01	0.01	0.05	0.03	n.d.	n.d.	0.05	0.04	0.02	0.06	0.03	0.03	n.d.	n.d.
Li	0.01	0.01	0.12	0.06	n.d.	n.d.	0.19	0.23	0.08	0.08	0.24	0.24	n.d.	n.d.
Fe ³⁺	0.44	0.08	0.71	0.80	1.02	0.85	1.90	1.48	1.42	1.34	1.24	1.19	0.66	0.72
Mg ²⁺	0.74	0.61	0.00	0.02	0.09	0.01	0.02	0.03	0.23	0.23	0.00	0.00	0.12	0.12
Fe ²⁺	3.42	3.53	3.76	3.92	3.60	3.87	2.35	2.76	2.85	2.96	2.95	2.86	3.78	3.77
Mn	0.07	0.06	0.11	0.06	0.11	0.10	0.12	0.12	0.09	0.08	0.17	0.16	0.14	0.14
Ca	1.75	1.77	0.04	0.04	0.41	0.28	0.16	0.11	0.20	0.25	0.02	0.03	0.18	0.21
Na	0.94	0.98	2.69	2.69	2.27	2.38	2.85	2.61	2.61	2.54	2.60	2.66	2.27	2.27
K	0.34	0.33	0.30	0.24	0.40	0.38	0.39	0.57	0.43	0.38	0.59	0.61	0.55	0.52
Zr	0.02	0.03	0.01	0.01	0.02	0.00	0.01	0.00	0.02	0.05	0.08	0.12	0.00	0.00
Cl	0.02	0.04	0.01	0.01	0.00	0.00	0.00	0.00	0.00	0.00	0.00	0.00	0.00	0.00
F	0.52	0.17	1.69	0.70	0.40	0.28	0.00	0.00	0.04	0.02	0.00	0.00	0.02	0.02
Sum	16.00	16.00	16.00	16.00	16.00	16.00	16.00	16.00	16.00	16.00	16.00	16.00	16.00	16.00

^a n.d. = not detected. Values are expressed as wt%.

bole. The latter is overgrown by some mm-thick coatings of aegirine visible by the naked eye.

3.1.7. Aegirine Vein (GM1257)

Millimeter- to cm-thick veins of aegirine, albite and analcime are abundant in the whole complex. They crosscut all other rock types and are therefore believed to represent products of late-stage hydrothermal fluids. Sample GM1257 is a compositionally zoned aegirine vein, which crosscuts naujaite (Fig. 3k). The margins of the vein are dominated by bottle-green needle-shaped aegirine growing towards the center of the vein, where albite and analcime are the dominant minerals. Similar aegirine-rich veins are known from other localities in the Gardar Province and have been described by Rønnevig and Dymek (1991).

3.2. Chemical Composition of the Ilímaussaq Amphiboles

Amphibole occurs in all major rock types as an early magmatic or interstitial mineral phase. It is thus suitable for Nd, O, and H isotope studies of magmatic processes. Major element compositions of amphiboles were determined using a JEOL

8900 electron microprobe at the Institut für Geowissenschaften of the Universität Tübingen, Germany. For calibration, both natural and synthetic standards were used. The beam current was 15 nA and the acceleration voltage was 15 kV. The counting time on the peak was 16 s for major elements, and 30–60 s for minor elements (Mn, Ti, Zr, F, Cl). Background counting times were half of the peak counting times. The peak overlap between the Fe L β and F K α lines was corrected for. To avoid Na migration under the electron beam, feldspar was analyzed using a defocused beam of 15 μ m diameter. Data reduction was performed using the internal $\phi\rho Z$ procedures of JEOL (Armstrong, 1991).

Li, Zn, and Zr contents were measured by in-situ laser ablation inductively coupled plasma-mass spectrometry (LA-ICP-MS) at the EU Large Scale Geochemical Facility (University of Bristol) using a VG Elemental PlasmaQuad 3 + S-Option ICP-MS equipped with a 266 nm Nd:YAG laser (VG MicroProbe II). Details of the method are described in Halama et al. (2002). Representative microprobe analyses of amphiboles from the different Ilímaussaq rocks are shown in Table 1. Amphibole formulae are based on 16 cations and 23 oxygens, assuming a completely filled A site.

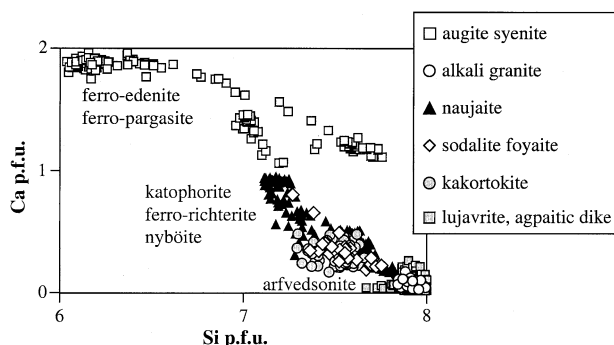


Fig. 4. Compositional range observed in the Ilímaussaq amphiboles plotted in a Ca p.f.u. vs. Si p.f.u. diagram according to Mitchell (1990).

Amphibole analyses from sample GM1212 have been published by Markl (2001b). Some further amphibole analyses from the Ilímaussaq rocks are found in Larsen (1976). Amphibole composition ranges from almost pure Ca-amphibole (ferroedenite, ferropargasite) in the early augite syenite via Na-Ca amphibole (katophorite, ferrichterite) to Na-amphibole (nyböite, arfvedsonite) in the agpaite rocks (Fig. 4). In the more evolved agpaite, amphibole has high contents of Li (up to 2500 ppm), Zn (5600 ppm), and Zr (5000 ppm) and evolves towards ferroleakeite composition. The major substitutions observed in this comagmatic suite are $\text{CaAl}^{\text{IV}} \leftrightarrow \text{NaSi}$ and $\square \text{Fe}^{3+} \leftrightarrow \text{Na}^{\text{A}}\text{Fe}^{2+}$ with a filling of the A site. Incorporation of Li occurs mainly according to $\text{Li} + \text{Fe}^{3+} \leftrightarrow 2(\text{Fe}^{2+}, \text{Mg}, \text{Mn})$ and $\text{Li} + \text{Fe}^{3+} \leftrightarrow \text{Al}^{\text{IV}} + \text{Na}$.

4. ISOTOPE GEOCHEMISTRY

4.1. Methods

Nd isotopic analyses were performed on ~10 mg of hand-picked mineral separates. They were spiked with ^{150}Nd - ^{149}Sm tracers before dissolution under high pressure in HF acid at 180°C in poly-tetrafluor-ethylene (PTFE) reaction bombs. Sm and Nd were separated and measured as described in Marks et al. (2003). The $^{143}\text{Nd}/^{144}\text{Nd}$ ratios were normalized to $^{146}\text{Nd}/^{144}\text{Nd} = 0.7219$, the Sm isotopic ratios to $^{147}\text{Sm}/^{152}\text{Sm} = 0.56081$. Analyses of 11 separate loads of Ames metal (Geological Survey of Canada, Roddick et al., 1992) during this study, gave a $^{143}\text{Nd}/^{144}\text{Nd}$ ratio of 0.512145 ± 24 ($\pm 2\sigma$ error of the mean), 11 loads of the La Jolla standard yielded a $^{143}\text{Nd}/^{144}\text{Nd}$ ratio of 0.511829 ± 30 . Total procedural blanks (chemistry and loading) were < 100 pg for Nd. A decay constant of $6.54 \times 10^{-12} \text{ a}^{-1}$ for ^{147}Sm (Lugmair and Marti, 1978) was used. $\epsilon_{\text{Nd}(T)}$ values were calculated using present-day CHUR values of 0.1967 for $^{147}\text{Sm}/^{144}\text{Nd}$ (Jacobson and Wasserburg, 1980) and 0.512638 for $^{143}\text{Nd}/^{144}\text{Nd}$ (Goldstein et al., 1984). Calculated uncertainty in $\epsilon_{\text{Nd}(T)}$ units based on analytical errors is not more than 0.5. Initial Nd isotope ratios of minerals were corrected for an age of 1160 Ma.

The oxygen isotope composition of the whole-rock sample GM1212 was determined using a modified version of the conventional method after Clayton and Mayeda (1963), with BrF_5 as reagent and converting the liberated oxygen to CO_2 before mass spectrometric analyses. The oxygen isotope com-

position of handpicked mineral separates was determined using a method adapted after Sharp (1990) and Rumble and Hoering (1994). Details of the method are described in Marks et al. (2003). The D/H ratios of amphibole separates and sample GM1212 were determined from ~100 to 200 mg of sample according to the method of Vennemann and O'Neil (1993) as well as on 2 to 4 mg sized samples according to a method adapted after Sharp et al. (2001).

Oxygen and hydrogen isotopic compositions were measured on a Finnigan MAT 252 isotope ratio mass spectrometer. Additional measurements of the hydrogen isotope compositions of minerals were made using high-temperature (1450°C) reduction methods with He-carrier gas and a TC-EA from Thermo-Finnigan linked to a Delta Plus XL mass spectrometer. The results are given in the standard δ -notation, expressed relative to VSMOW in permil (‰). Replicate oxygen isotope analyses of the standards (NBS-28 quartz and UWG-2 garnet; Valley et al., 1995) had an average precision of $\pm 0.1\text{‰}$ for $\delta^{18}\text{O}$ values. The precision of the in-house kaolinite standard and NBS-30 biotite for hydrogen isotope analyses was better than $\pm 2\text{‰}$ for both H-isotope methods used; all values were normalized using a value of -125‰ for this kaolinite standard and -65‰ for NBS-30 analyzed during the same period as the amphiboles.

Water content for some samples was estimated independently as part of the hydrogen isotope analyses (e.g., Vennemann and O'Neil, 1993). However, the estimates for most samples must be considered as minimum estimates only as the amphibole separates were not pure in all cases, containing variable amounts of pyroxene as the major anhydrous contaminant.

4.2. Sm-Nd Systematics

12 mineral separates from 10 samples and one whole-rock sample (GM1212) were analyzed for their Sm and Nd concentrations and their Nd isotopic compositions (Table 2). The range in Sm (0.4 to 84 ppm in amphibole, 596 ppm in whole-rock) and Nd (3.9 to 432 ppm in amphibole, 4760 ppm in whole-rock) concentrations is relatively large. The lowest concentrations were found in minerals of an agpaite pegmatite (GM1390), the highest concentrations were measured in the agpaite dike whole rock sample (GM1212).

Figure 5 shows the Sm-Nd isotopic data in a conventional isochron diagram. The data define a single isochron. Two separates of amphibole from alkali granites and the agpaite dike rock show the most pronounced deviations from the general trend in that they are shifted to significantly lower and higher $^{143}\text{Nd}/^{144}\text{Nd}$ ratios, respectively. Omitting these data, an age of 1160 ± 30 Ma is obtained for the remaining data, which is in agreement with previous age data (Blaxland et al., 1976; Paslick et al., 1993; Waight et al., 2002).

Overall, the Ilímaussaq samples range from $\epsilon_{\text{Nd}(T)} = -0.1$ to -3.1 with the lowest value in the alkali granite (Fig. 6). Two mineral separates of the augite syenite (augite, amphibole) yield indistinguishable values of about -1 . The calculated $\epsilon_{\text{Nd}(T)}$ values for agpaite are identical within analytical error and span a small range between $\epsilon_{\text{Nd}(T)} = -1.1$ and -1.8 . Minerals from the late-stage samples GM1257 and GM1390 have relatively high $\epsilon_{\text{Nd}(T)}$ values between -0.1 and -0.5 .

Table 2. Sm-Nd data and oxygen and hydrogen isotope compositions for mineral separates and one whole rock sample of the Ilfmaussaq intrusion.^a

Sample	Rock type	Mineral	Sm (ppm)	Nd (ppm)	¹⁴⁷ Sm/ ¹⁴⁴ Nd	¹⁴³ Nd/ ¹⁴⁴ Nd	$\epsilon_{Nd(1160)}$	T_{DM} (Ga)	$\delta^{18}O$ (‰)	wt% water	Zinc-method	δD (‰)	TC-EA	n for TC-E
GM1330	Augite syenite	Amphibole	83.67	431.6	0.1172	0.511987 (08)	-0.9	1.78	5.7	0.78	-92			
GM1330	Augite syenite	Augite	22.1	91.23	0.1464	0.512193 (10)	-1.2	1.80	5.6					
GM1330	Augite syenite	Olivine							5.3					
GM1303	Alkali granite	Amphibole	13.43	72.6	0.1119	0.511832 (09)	-3.1	1.96	5.6	0.75	-232	-183	6	
GM1214	Sodalite foyaite	Amphibole	8.602	58.19	0.0894	0.511765 (09)	-1.1	1.79	5.7	1.02	-150			
GM1370	Naujaite	Amphibole	10.47	63.61	0.0995	0.511847 (12)	-1.0	1.79	5.4		-198			
GM1335	Kakortokite (red)	Amphibole	6.115	35.74	0.1034	0.511838 (09)	-1.8	1.85	5.3	1.13	-171	-173	6	
GM1337	Kakortokite	Amphibole	4.190	26.76	0.0947	0.511783 (07)	-1.5	1.83	5.5	0.98	-171	-179	3	
GM1843	Lujavrite	Amphibole	14.23	80.1	0.1074	0.511884 (10)	-1.4	1.82	5.5	1.27	-132			
GM1257	Aegirine vein	Aegirine	7.970	41.99	0.1148	0.511991 (10)	-0.5	1.74	5.6					
GM1212	Exsolved lujavrite	Whole rock	595.5	4763	0.0756	0.511648 (10)	-1.3	1.81	5.6					
GM1390	Agpaitic pegmatite	Aegirine	0.822	5.390	0.0922	0.511835 (12)	-0.1	1.72	5.2					
GM1390	Agpaitic pegmatite	Amphibole	0.401	3.898	0.0622	0.511587 (14)	-0.5	1.75	5.4					
GM1849	Agpaitic dike	Amphibole	15.46	90.51	0.1033	0.511965 (08)	+0.7	1.65	4.5					
GM1849	Agpaitic dike	Olivine						1.65	4.5					

^a Errors of measured ¹⁴³Nd/¹⁴⁴Nd are given as 2σ values and are indicated in parentheses. Calculation of Nd-model ages according to Liew and Hofmann (1988).

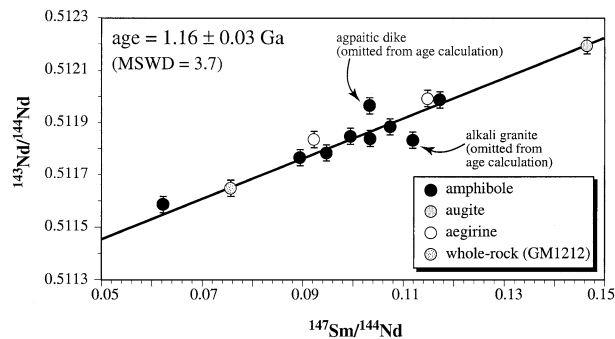


Fig. 5. Sm-Nd isotope diagram for all analyzed mineral separates (amphibole, aegirine, augite) and whole rock sample GM1212. Note that an isochron age of 1160 ± 30 Ma was calculated omitting the data for amphibole separates from the alkali granite (GM1303) and the agpaitic dike rock (GM1849).

Amphibole from the micro-kakortokite dike (GM1849) has a positive $\epsilon_{Nd(T)}$ value of +0.7. Nd-model ages (Liew and Hofmann, 1988) range between 1.65 and 1.96 Ga with the youngest value calculated for amphibole from the agpaitic dike (GM1849) and the oldest value for amphibole from the alkali granite (GM1303).

4.3. Oxygen and Hydrogen Isotope Compositions

Measured $\delta^{18}O$ and δD values are presented in Table 2. The $\delta^{18}O$ values of all samples range between +4.6 and +5.7‰ with the lowest value obtained for amphibole of the agpaitic dike rock GM1849. All other amphiboles have similar values between +5.3 and +5.7‰ (Fig. 6). $\delta^{18}O$ values measured for aegirine, olivine, augite, and the whole-rock sample GM1212 fall in the range of measured values for amphiboles.

δD values for amphibole separates and the whole-rock sample GM1212 are between -232 and -92‰. In general, the agreement between the two methods used for hydrogen isotope

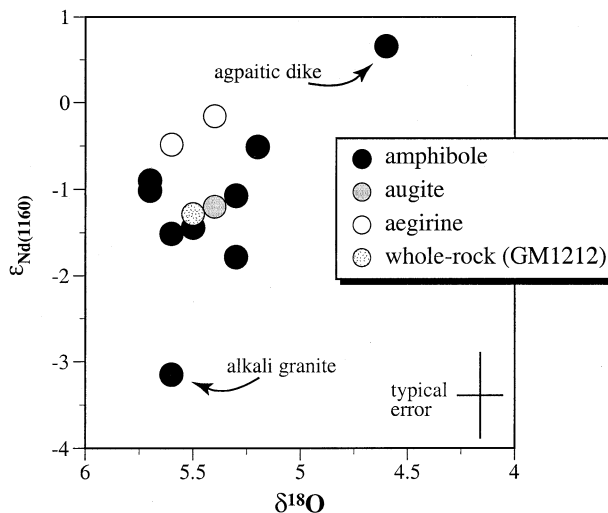


Fig. 6. Measured $\delta^{18}O$ versus calculated $\epsilon_{Nd(1160)}$ values for Ilfmaussaq mineral separates. Note the two outliers (alkali granite and agpaitic dike rock) from the majority of the data set.

analyses is within ~ 10 to 15‰, except for the sample of the alkali granite where the values differed by more than 50‰. This sample also had the lowest measured amphibole value from the present suite of rocks, the highest was measured in amphibole from the augite syenite; the agpaitic samples fall within this range. The reason for the slight to large discrepancies in values between the two methods is unknown, but may be related to significant heterogeneity of H-isotopic compositions of the samples and the different amounts of samples used for the methods. Significant heterogeneity of δD values may also be indicated by the replicate analyses of amphiboles using the TC-EA method, as the values given in Table 2 represent average values of 6 individual measurements with standard deviations that were significantly worse ($\pm 4\%$) than those for the standards used. However, these standard deviations do not at all prohibit to draw the conclusions detailed below. Furthermore, large hydrogen isotopic heterogeneities in individual, magmatic amphiboles have been described before, for example by Déloule et al. (1991). With the exception of amphibole from the augite syenite, the hydrogen isotope compositions are among the most D-depleted igneous amphiboles yet recorded (cf. Sheppard, 1986a).

5. DISCUSSION

5.1. Magma Source and Evolution

Excluding the amphibole from the agpaitic dike (GM1849), the similarity in oxygen isotope compositions of the minerals implies a parental melt that is homogeneous with respect to oxygen isotopes. The small fractionation between augite (+5.6‰) and olivine (+5.3‰) in the augite syenite (GM1330) is typical for high temperature equilibrium. Because mineral-melt fractionations at magmatic temperatures are small for olivine, augite, and amphibole (Taylor and Sheppard, 1986; Matthey et al., 1994) and because these minerals are known to have high closure temperatures for oxygen diffusion (Farver and Giletti, 1985; Farver, 1989; Gérard and Jaoul, 1989), the estimated $\delta^{18}O_{\text{melt}}$ values for all Ilímaussaq melt(s) is $\sim 6.0\%$. This value is well within the range typical for syenitic bodies (e.g., Taylor and Sheppard, 1986; Lutz et al., 1988; Harris, 1995; Dallai et al., 2003) and supports a principle mantle derivation of the magmas (cf. Kyser, 1986; Eiler, 2001). The O-isotopic composition of feldspars was not measured in this study, owing to the difficulty of separating clean, unaltered feldspar from the samples used.

The oxygen isotope compositions of olivine and amphibole in the agpaitic dike (GM1849) are reversed, with olivine also having a $\delta^{18}O$ value compatible with a typical mantle-derivation of the melt, but that of the late-stage amphibole (4.6‰; Table 2) indicating influence of contamination with a source low in ^{18}O . As the agpaitic dike also has a distinct Nd-isotopic composition and calculated Fe^{3+}/Fe^{2+} ratio (Fig. 9) compared to the other samples, late-stage magmatic contamination for this sample is indicated. On the basis of the present data, the contamination may also have been mediated through an exchange with meteoric water. This indicates that a late-stage alteration in isotopic compositions can be evidenced by O- and Nd-isotopic compositions. This dike and its origin relative to

the other rocks is discussed in more detail in Marks and Markl (2003).

The oxygen isotope compositions measured for amphiboles in this study are, however, quite different from those reported for Ilímaussaq amphiboles by Konnerup-Madsen (1980) and Sheppard (1986a), who measured $\delta^{18}O$ values between +7 and +8.4‰. They also reported $\delta^{18}O$ values for feldspars of between 5.8 to 9.3‰, and values of 9.2 to 9.3‰ for quartz in the alkali granite and quartz syenite. These relatively high $\delta^{18}O$ values as well as high $^{87}Sr/^{86}Sr$ initial ratios for the Ilímaussaq agpaites (Blaxland et al., 1976), lead Sheppard (1986a) to suggest that the Ilímaussaq magmas must have been contaminated by crustal material, either through crustal anatexis or during emplacement of the magma. The reason for the large discrepancy in measured $\delta^{18}O$ values of the amphiboles is unclear to us, but may relate to the different analytical techniques employed. Measurements of oxygen isotope compositions using conventional fluorination of silicates in nickel-vessels compared to laser-based fluorination techniques have been noted to give quite different results for olivine and pyroxene from the same mantle peridotites, with conventional analyses commonly providing higher $\delta^{18}O$ values and a much wider range in values for peridotites (cf. Kyser et al., 1981; Matthey et al., 1994; and summary in Eiler, 2001). Similar differences, although not measured in the same rocks, have been noted for amphiboles from hydrous peridotites (e.g., Bottcher and O'Neil, 1980; Chazot et al., 1997). This, however, would not explain the group of feldspars with high $\delta^{18}O$ values. Given that the feldspar values reported by Sheppard (1986a) do not simply reflect late-stage alteration but instead are taken to be representative of magmatic compositions, they are difficult to reconcile with the $\delta^{18}O$ values measured for the amphiboles, olivines and pyroxene from this study, in particular because the review by Sheppard (1986a) does not provide further details on sampling sites or mineral paragenesis. However, the petrographic appearance of feldspars as observed in the rocks of this study as well as an obvious disequilibrium between the O-isotope compositions reported for coexisting feldspar-amphibole or feldspar-quartz pairs in three rocks reported by Konnerup-Madsen (1980), may indicate that at least some of their samples have been affected by late-stage alteration. If so, it is of interest to note that this alteration may have led to a relative increase in the ^{18}O -content of the minerals compared to minerals crystallized from normal mantle-like melts, hence arguing against late-stage infiltration of low- $\delta^{18}O$ meteoric water.

On the basis of initial Sr-isotope compositions of the augite syenite (~ 0.703) and the agpaitic rocks (~ 0.710), Blaxland et al. (1976) suggested derivation of the augite syenite and the agpaites from primitive mantle material, but with preferential leaching of radiogenic strontium from crustal material by the agpaitic melt. This interpretation is not in contradiction with our model since fluid mobility of Rb and Sr is known from whole-rock studies in general (e.g., Ashwal et al., 2002) and from mineral studies from other alkaline rocks in the Gardar province (e.g., Marks et al., 2003). Effects of this kind on the Sm-Nd system are expected to be much smaller.

Similar to the oxygen isotope compositions measured in this study, the Nd isotope compositions are also homogeneous (Fig. 6). With the exception of amphibole from the alkali granite and from the agpaitic dike, the initial $\epsilon_{Nd(T)}$ values overlap within

Table 3. Oxygen and neodymium isotopic compositions and Nd concentrations of possible contaminants for the Ilímaussaq alkali granite.

Potential contaminant	$\delta^{18}\text{O}$ (‰)	ϵ_{Nd} (1160 Ma)	Nd (ppm)	Reference
Julianehab batholith	+7.8	-8.3	62	Halama (in press)
Eriksfjord sandstones	+11.5	-7	7	Andersen (1997); Halama et al. (2004)
Archaean lower crust	+7.5	-23.4	63	Taylor et al. (1984); Fowler and Harmon (1990)

analytical error and are similar to most of the whole-rock data from Stevenson et al. (1997) and mineral data from Paslick et al. (1993). Furthermore, there is no significant difference in $\epsilon_{\text{Nd(T)}}$ values between amphibole separates of the major rock types and amphibole of late-stage samples. The observed homogeneity implies a closed system during the evolution of the Ilímaussaq melts. Even during late-stage crystallization in pegmatites and hydrothermal veins, no major influence of an external source can be detected.

On the basis of whole rock Nd-isotopic compositions, Stevenson et al. (1997) calculated decreasing proportions of assimilation from the augite syenite to the agpaitic rocks. In contrast, if we assume a homogeneous mantle source and closed system behavior during crystallization for most of the Ilímaussaq melts and late-stage pegmatites and veins, our Nd data would indicate a mantle source slightly enriched in ^{18}O and depleted in ^{147}Sm compared to the bulk mantle. The occurrence of contaminated samples at the margins of the complex shows that significant assimilation of country rock occurred only on a local scale (Ferguson, 1964; Stevenson et al., 1997; Marks and Markl, 2001). Whereas Stevenson et al. (1997) believe that the parental melt for the Ilímaussaq rocks was derived from a depleted mantle, we favor a model where the Ilímaussaq rocks are derived from a mantle source depleted in ^{147}Sm compared to normal mantle values, either because of mantle metasomatism before melting (Upton, 1987; Goodenough et al., 2002) or because the mantle source had been modified by plume material (Zindler and Hart, 1986; Nicholson and Shirey, 1990; Halama et al., 2003).

There are two significant outliers in the present data set of Nd isotopic compositions: amphibole from the alkali granite has a lower $\epsilon_{\text{Nd(T)}}$ value of -3.1, whereas amphibole from the agpaitic dike rock has a positive $\epsilon_{\text{Nd(T)}}$ value of +0.7. The origin of the alkali granite can be explained by significant amounts of crustal contamination (see below). The more positive $\epsilon_{\text{Nd(T)}}$ value for the agpaitic dike rock implies less contamination with low $\epsilon_{\text{Nd(T)}}$ material for this dike rock and is discussed in more detail in Marks and Markl (2003).

The less radiogenic $\epsilon_{\text{Nd(T)}}$ value of the alkali granite has been explained by extensive contamination of the basaltic or augite syenite magma with assimilated country rocks (Stevenson et al., 1997). Potential contaminants to explain the quartz-saturated alkali granite include sandstones of the Eriksfjord formation, the surrounding Julianehåb granite, or lower crustal rocks that, however, are not exposed at the present surface but may occur beneath the Julianehåb batholith (Dahl-Jensen et al., 1998). Table 3 summarizes oxygen and neodymium isotopic data and Nd concentrations for possible contaminants. A concentration of 80 ppm Nd (Bailey et al., 2001) is used as an approximation for the augite syenite melt. For the granitic upper crust, a typical Julianehåb granite sample from the vi-

cinity of the complex is used (Halama et al., 2004). Neodymium and oxygen isotope data for sandstones of the Eriksfjord Formation are from Andersen (1997) and from Halama (unpublished data), respectively. For a potential lower crust, oxygen data from Fowler and Harmon (1990) and neodymium data from siliceous Archaean gneisses (Taylor et al., 1984) provide an approximation. If we apply a two-component mixing model (Pushkar et al., 1972), the amount of these potential contaminants necessary to explain the neodymium isotopic composition of the alkali granite via contamination of the augite syenitic melts can be calculated using the following equation:

% amount of contaminant

$$= \frac{C_{\text{Nd}}^{\text{augitesyenite}} * (\epsilon_{\text{Nd}}^{\text{alkaligranite}} - \epsilon_{\text{Nd}}^{\text{augitesyenite}})}{C_{\text{Nd}}^{\text{contaminant}} * (\epsilon_{\text{Nd}}^{\text{contaminant}} - \epsilon_{\text{Nd}}^{\text{alkaligranite}})} \quad (1)$$

Using this formula, it appears, that sandstones of the Eriksfjord Formation are not valid as a potential contaminant because of their very low Nd concentration. For the granitic upper crust the amount of bulk assimilation was calculated to be ~60%, which appears unrealistic for energetic reasons. Furthermore, such high amounts of assimilation would result in $\delta^{18}\text{O}_{\text{melt}}$ -values of ~7‰, which is not compatible with the measured mineral data. However, bulk assimilation of ~13% of lower crust would explain the neodymium isotopic composition of the alkali granite and would result in a $\delta^{18}\text{O}_{\text{melt}}$ -value of 6.2‰, which is in the range of calculated $\delta^{18}\text{O}_{\text{melt}}$ -values. Our preferred interpretation, therefore, is that during ascent of the augite syenite magma, parts of it became contaminated with lower crustal melts and thereby reached quartz-saturation.

In summary, the preferred interpretation of the mineral O- and Nd-isotopic compositions is that the whole complex, with the exception of the alkali granite, evolved from a rather homogeneous magma in a closed system without significant contamination during ascent, emplacement, cooling, and final crystallization of the different melt batches.

The measured oxygen isotopic compositions of the amphiboles (Table 2) can be used to calculate the isotopic composition of a coexisting fluid phase. Amphibole-water oxygen isotope fractionation between 500° and 800°C is approximately -1 to -2‰ (Zheng, 1993), indicating a relatively homogeneous oxygen isotopic composition of the fluid of +6.3 to +7.6‰. The calculated fluid of the agpaitic dike has a relatively low $\delta^{18}\text{O}$ value of +5.4 to +6.4‰. All of these fluid $\delta^{18}\text{O}$ values are typical for magmatic fluids (e.g., Sheppard, 1986b; Hoefs, 1997).

5.2. Discussion of the Hydrogen Isotope Compositions

With the exception of amphibole from the augite syenite, the hydrogen isotope compositions measured for amphiboles from

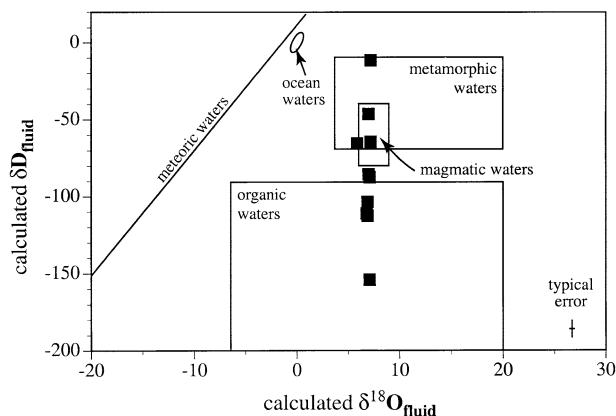


Fig. 7. Calculated $\delta^{18}\text{O}_{\text{fluid}}$ and $\delta\text{D}_{\text{fluid}}$ values for the Ilímaussaq complex based on present mineral- H_2O fractionations (see discussion). Fields for ocean water, meteoric waters, primary magmatic waters, metamorphic waters, and organic waters are from Sheppard (1986b) and shown for comparison.

Ilímaussaq in this study, as well as the previous measurements reported by Konnerup-Madsen (1980) and Sheppard (1986a) are well off the range typical for amphiboles in igneous rocks ($\delta\text{D} = -80$ to -40‰ ; e.g., Hoefs, 1997) and are among the most D-depleted igneous amphiboles yet recorded. Arfvedsonites with similarly low δD values have been measured from rocks of the peralkaline Red Wine Complex, Labrador, (-160‰ ; Sheppard, 1986a) and from nepheline syenites of the Norra Kärr Intrusive Complex, Sweden (-130‰ and -150‰ ; Sheppard, 1986a), as well as from Lovozero, Russia (-130‰ ; Vennemann and Potter, unpublished data) and Khibina, Russia (-110‰ ; Vennemann and Potter, unpublished data). These low values may hint at a common process that controls the hydrogen isotope compositions of amphiboles in peralkaline to agpaitic rocks.

Explanations proposed for low δD values of amphiboles from magmatic rocks include:

1. Exchange with meteoric-hydrothermal fluids either during magmatic intrusion and/or as subsolidus exchange after crystallization of the magma (e.g., Taylor, 1974; Neve et al., 1994; Brandriss et al., 1995; Agemar et al., 1999).
2. Extreme magmatic degassing of water (e.g., Nabelek et al., 1983; Taylor et al., 1983)
3. Lack of appropriate mineral-water fractionation factors for Fe-rich minerals and/or pressure effects on the mineral water H-isotope fractionation (e.g., Suzuoki and Epstein, 1976; Graham et al., 1984; Vennemann and O'Neil, 1996; Driesner, 1997; Chacko et al., 2001).
4. Assimilation of organic-rich sediments and/or exchange with fluids derived from organic matter (e.g., Sheppard, 1986a)

The Ilímaussaq rocks of the present study show no mineralogical evidence for an extensive meteoric low-temperature alteration. This is confirmed for the amphiboles by their oxygen isotope compositions as measured in this study (Fig. 7), with the exception of the sample from the agpaitic dike, which has both unusual O- and Nd-isotopic compositions. The values for the dike indicate that a late-stage alteration in isotopic compositions can indeed be evidenced by O- and Nd-isotopic compositions. Also, as was already argued by Sheppard (1986a),

the relatively high $\delta^{18}\text{O}$ values for feldspars and the not unusual δD values of the surrounding volcanic rocks of the Eriksfjord Formation (values of around -80‰ ; Sheppard, 1986a) do not provide support for hydrothermal circulation of low- δD meteoric fluids during or shortly after emplacement of the magmatic rocks.

Major magmatic degassing as an explanation for the low δD values is also not considered viable, both on the basis of estimated water contents for the different magmatic rocks given as by Bailey et al. (2001) and on the basis of the present data set, because there is no correlation between water content of the rock or mineral and the δD values of amphibole. Correlations with exponentially decreasing δD values as a function of decreasing water content in the magmatic rocks or constituent minerals characterizes degassing of water according to Rayleigh-type principles (Nabelek et al., 1983; Taylor et al., 1983), which is not observed in this study (Fig. 8). Furthermore, extreme loss of water such as would be required to obtain the extremely low δD values in residual melts or minerals, would destabilize the formation of late-formed amphibole.

Preferential degassing of molecular H_2 , in contrast to water, is a common mechanism for the oxidation of magmatic liquids (Sato, 1978; Mathez, 1984) and can lead to increasing enrichment in D in the residual phases (e.g., Kyser, 1986). An increase in the oxidation state of the melt may occur by redox reactions such as:

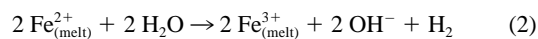


Figure 9 shows the range of observed $\text{Fe}_{(\text{tot})}$ and calculated $\text{Fe}^{3+}/\text{Fe}^{2+}$ ratios in amphiboles of the different rock types versus the measured δD value. With the exception of amphiboles from the alkali granite, these parameters show weak inverse correlations. If the $\text{Fe}^{3+}/\text{Fe}^{2+}$ ratio of the amphiboles

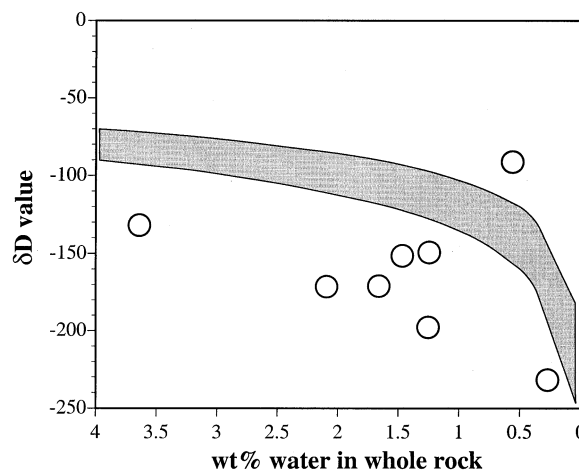


Fig. 8. The correlation of δD values as a function of decreasing water content in the magmatic rocks according to Rayleigh-type principles (Nabelek et al., 1983; Taylor et al., 1983) assuming an initial water content for the Ilímaussaq melts of 4 wt% (Larsen and Sørensen, 1987). The gray field represents the calculated curves for an typical initial water δD value of -70 to -90‰ (Hoefs, 1997) and a $1000\ln\alpha_{\text{melt-H}_2\text{O}}$ value of -25 to -35‰ . White dots represent the estimated water contents for the different magmatic rocks of the Ilímaussaq complex and the agpaitic dike rock (Larsen and Steenfelt, 1974; Bailey et al., 2001).

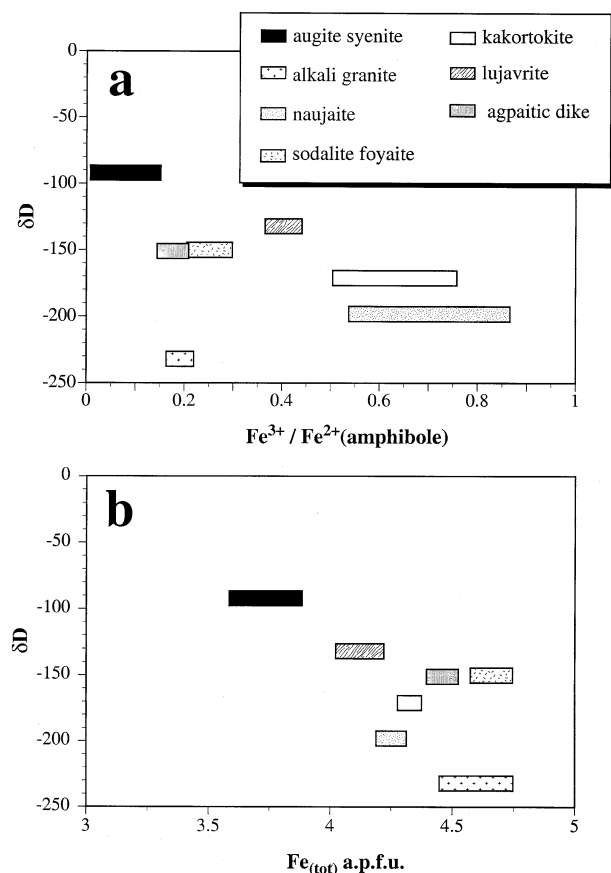


Fig. 9. (a) Range of calculated $\text{Fe}^{3+}/\text{Fe}^{2+}$ ratios versus δD value for amphiboles of the different rock types. The box for each sample represents the whole variation found for this sample on the basis of microprobe analyses. With the exception of amphiboles from the alkali granite these parameters show an inverse correlation. (b) $\text{Fe}_{(\text{tot})}$ a.p.f.u. (atoms per formula unit) of amphiboles versus δD values of the different rock types. A rough correlation between these two parameters can be recognized.

directly reflects the oxidation state of the parental melt, the augite syenite melt was more reduced than the agpaitic and the alkali granite melts. This is in good accordance with petrological results (Larsen, 1976; Markl et al., 2001) and fluid inclusion studies (see below). During fractionation and cooling of the melt, the water content increased supporting progress of reaction (2). The oxidation of ferrous iron into its ferric state may have released molecular hydrogen, which would be depleted in deuterium relative to water (around 200‰ at 700°C; Horibe and Craig, 1995). Hence, if significant degassing of H_2 occurs during melt crystallization and formation of amphibole at increasingly oxidizing conditions, δD values of amphibole should actually increase with increasing $\text{Fe}^{3+}/\text{Fe}^{2+}$ ratios. Even though the correlation between $\text{Fe}^{3+}/\text{Fe}^{2+}$ and δD value is fairly weak, particularly given the potential errors involved in estimating $\text{Fe}^{3+}/\text{Fe}^{2+}$ ratios from electron microprobe data (e.g., Cosca et al., 1991; Feldstein et al., 1996), this relationship suggests that internal buffering mechanisms and accompanying loss of H_2 is neither a viable process to account for the change in δD values, nor for the low δD values. It is also of interest to note that the amphibole from the agpaitic dike, which has a

distinctly lower $\delta^{18}\text{O}$ value and Nd-isotopic composition, also falls off the trend in δD vs. $\text{Fe}^{3+}/\text{Fe}^{2+}$ ratios, suggesting equilibration with a fluid of somewhat different composition compared to the other samples.

To calculate the composition of a fluid phase, which has subsequently been removed from the original mineral-fluid system, it is necessary to know the isotopic fractionation factors between hydrous minerals and fluid. Variables that influence the magnitude of fractionation factors include temperature, pressure, mineral composition, and fluid composition (cf. O'Neil, 1986; Chacko et al., 2001; and references therein). However, for some important mineral-water H-isotope systems major discrepancies exist between different experimental calibrations and raise questions about the validity of some of the published fractionation curves if extrapolated to extreme compositions, temperatures or pressures. The amphibole-water hydrogen isotope fractionations as given by Suzuoki and Epstein (1976) and Graham et al. (1984), which show a reasonable agreement for Fe-poor compositions, are in obvious disagreement on the effects of Fe on mineral-water fractionations. The reasons for the disagreement are not known, but at least some of the differences may relate to differences in pressures used for the experiments (Driesner, 1997; Horita et al., 1999; Chacko et al., 2001). Using a maximum pressure correction for the Ilímaussaq samples, which may be applicable as the intrusion depths are fairly shallow, calculated δD values of water in equilibrium with the amphiboles would shift by +30‰ (Driesner, 1997; Horita et al., 1999), still extending towards values unlike those for typical magmatic waters (Fig. 7). The rough negative correlation between $\text{Fe}_{(\text{tot})}$ of amphiboles and the measured δD values (Fig. 9) supports the conclusions on effects of Fe on D-H fractionations between minerals and water by Suzuoki and Epstein (1976) in principle. However, given the general mineral-water calibration of Suzuoki and Epstein (1976) that relates the fractionation factor to the composition of the minerals, the calculated variation in $1000\ln\alpha_{\text{amph-water}}$ for the present minerals amounts to ~13‰ only. This is much smaller than the observed variation in δD values of the amphiboles and, given the relatively small differences in Fe-content between the amphiboles of this study but the large variation between their δD values, also appears to be an unlikely explanation for the large range in δD values measured in this study. Hence, unless the effect of Fe is much stronger than previously thought, the present data would still argue for significant heterogeneity in the H-isotopic composition of the fluid. More experimental work on pressure effects and the Fe-dependency of mineral-water fractionation factors under specified pressures is needed to solve this discrepancy between existing mineral-water H-isotope fractionations.

For the very Fe-rich amphiboles of Ilímaussaq (Table 1) amphibole-water hydrogen isotope fractionation at final equilibration temperatures of 350°C can be as large as about -65 to -77‰ (expressed as $1000\ln\alpha_{\text{amph-water}}$) according to the equation of Suzuoki and Epstein (1976) for the given mineral compositions (Table 1), or as low as -23‰ according to the calibration of Graham et al. (1984). Using, as a maximum estimate for the D/H ratios of water, the amphibole-water hydrogen isotope fractionations of Suzuoki and Epstein (1976), the δD values calculated for water in equilibrium with the amphiboles of this study at 350°C are extremely heteroge-

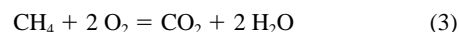
neous: -12% (augite syenite), -43 to -116% (agpaitic rocks) and -154% (alkali granite). Figure 7 shows the calculated $\delta^{18}\text{O}_{\text{fluid}}$ and $\delta\text{D}_{\text{fluid}}$ values relative to ranges typical for ocean water, meteoric waters, primary magmatic waters, metamorphic waters, and waters that exchanged with or originated from organic matter (Sheppard, 1986b). The observed heterogeneity and the exceptionally low calculated $\delta\text{D}_{\text{fluid}}$ values are in direct contrast to the rather homogeneous $\delta^{18}\text{O}$ values. This indicates that these two isotope systems are largely decoupled and may suggest, that H-bearing molecules other than water are responsible for the variance and low δD values.

On the basis of the low δD values, the high $\delta^{18}\text{O}$ values measured with conventional methods, and the initial $^{87}\text{Sr}/^{86}\text{Sr}$ for Ilímaussaq rocks, Sheppard (1986a) preferred the interpretation that the magmas have been contaminated with or at least influenced by fluids derived from organic-rich sediments. However, in view of the new results of this study we believe that contamination of the Ilímaussaq intrusion has played a minor role only and is not a viable model to explain the new results obtained in this study. According to the oxygen and neodymium isotope data of minerals presented in this study, upper crustal contamination of the magmas appears to be limited, allowing for relatively small amounts of a H-rich contaminant such as an organic-rich sediment only. An organic-rich contaminant is presently not known to occur in the Gardar province anyway. Furthermore, such a contaminant would also be expected to influence the C-isotopic composition of fluids in the late magmatic system.

Typical for such agpaitic igneous rocks is the existence of an exsolved CH_4 -dominated fluid phase. Various fluid inclusion studies (Larsen, 1976; Konnerup-Madsen et al., 1979, 1988; Konnerup-Madsen and Rose-Hansen, 1984; Konnerup-Madsen, 2001; Markl et al., 2001) showed that, with the exception of the alkali granite, primary fluid inclusions of the Ilímaussaq rocks are methane-dominated with lesser amounts of H_2 and higher hydrocarbons, but with only traces of H_2O and CO_2 . Similar hydrocarbon-rich fluids have been described from other peralkaline complexes worldwide (e.g., Salvi and Williams-Jones, 1997; Potter et al., 1998). The observed distribution and type of hydrocarbon inclusions (Konnerup-Madsen, 2001) combined with the stable isotope compositions of methane in the fluid inclusions, point to an abiogenic origin of methane with H- and C-isotopic compositions typical for magmatic systems rather than an organic contaminant (Konnerup-Madsen et al., 1988), which is also in agreement with the very reduced mineral assemblages (Markl et al., 2001). Stable isotope measurements of methane extracted from fluid inclusions provided δD values between -132 and -145% (Konnerup-Madsen et al., 1988; Konnerup-Madsen, 2001), which are very similar to isotopic compositions measured for fluid inclusions from the alkaline igneous rocks of the Lovozero Massif (δD values of methane between -132 and -167% ; Nivin et al., 1995). Hence, similar conclusions can be drawn from fluid inclusion studies of other alkaline intrusions of this type (e.g., Potter et al., 1998). Water calculated to be in equilibrium with this methane has a δD value of about -65 to -75% (Richet et al., 1977; Horibe and Craig, 1995), which is within the range of values typical for magmatic water (e.g., Sheppard 1986b; Hoefs, 1997).

Our preferred interpretation to explain both the low δD

values as well as the results of the fluid inclusion studies of the Ilímaussaq rocks without significant contamination from extraneous sources is the oxidation of magmatic methane. During late-magmatic cooling, the oxidation state of the whole system increases (Markl et al., 2001) and primary magmatic methane is oxidized according to the following schematic reaction.



An increase in the oxidation state for the Ilímaussaq rocks to values as high as the hematite-magnetite buffer during late-magmatic conditions is indicated, for example, by the formation of aegirine at the expense of arfvedsonite (Markl et al., 2001). The formation of aegirine in similar rocks of the Puklen intrusion, South Greenland (Marks et al., 2003) was shown to occur at temperatures down to 300°C . If CH_4 is quantitatively oxidized, water formed from such methane would have the H-isotopic composition of the precursor methane, which was analyzed to be about -140% . Reequilibration in this temperature range of primary arfvedsonite with this H-depleted water would result in H-isotopic compositions for amphibole down to about -220% (using the fractionations of Suzuoki and Epstein at 350°C for the given amphibole compositions), which covers the range of measured δD values. This process requires secondary exchange of hydrogen isotopes between amphiboles and the methane-dominated fluid and/or water derived from such methane. Such secondary exchange between earlier crystallized minerals and late-stage fluids that may even be internally generated has previously been suggested to account for a large range in δD values of amphiboles in a number of volcanic rocks (e.g., Miyagi et al., 1998; Miyagi and Matsubaya, 2003).

It is also worth noting that a number of authors suggested that the formation of hydrocarbons could be related to late- or postmagmatic alteration of Fe-rich minerals resulting in the production of H_2 (e.g., Salvi and Williams-Jones, 1997; Potter et al., 1998). For the Strange Lake peralkaline complex (Salvi and Williams-Jones, 1997) and for Khibina and Lovozero (Potter et al., 1998; Potter, 2002) textural evidence was interpreted to support a secondary origin of CH_4 -dominated fluid inclusions, leading to the suggestion that these reduced fluids formed during late hydrothermal activity. The released molecular hydrogen is strongly depleted in D compared to methane or water (Horibe and Craig, 1995). By analogy to the oxidation of methane, such hydrogen must be quantitatively oxidized to water before secondary reequilibration with primary amphibole to account for the observed variation in Fe content and $\text{Fe}^{3+}/\text{Fe}^{2+}$ in the present rocks and because the mineral-hydrogen fractionation factors are also extremely large (Vennemann and O'Neil, 1996). In the Ilímaussaq rocks, however, CH_4 -dominated fluid inclusions are undoubtedly of primary origin (Konnerup-Madsen and Rose-Hansen, 1984; Konnerup-Madsen, 2001).

6. CONCLUSIONS

The neodymium and oxygen isotope data of mineral separates of the Ilímaussaq intrusion indicate that most of the Ilímaussaq melts are derived from an isotopically homogeneous mantle source. Because there are no significant differences in $\delta^{18}\text{O}$ values or Nd isotopic composition between early magmatic and late-stage to hydrothermal minerals, a closed

system behavior during crystallization and cooling can be assumed for the Ilímaussaq melts. The neodymium isotope data are interpreted to reflect a mantle source with initial ϵ_{Nd} values of about -1 to -2 . The oxygen isotope composition of the Ilímaussaq melts is estimated to be around $+5.7$ to 6.0% . The alkali granite unit of the Ilímaussaq complex has the same oxygen isotopic composition but a less radiogenic neodymium isotope composition ($\epsilon_{\text{Nd}(T)} = -3.1$) compared to the other samples. On the basis of the presently known Nd- and O-isotope compositions and Nd concentrations higher amounts of assimilation of granitic basement rocks or sandstones are ruled out. Limited contamination with lower crustal rocks during ascent of the alkali granite is probably responsible for this contrast.

The wide variation in δD values is in contrast to the homogeneous O- and Nd-isotopic compositions as measured for splits of the same minerals in this study. The present results, together with whole rock δD values from surrounding country rocks (Sheppard, 1986a) and studies of the chemical and isotopic compositions of fluid inclusion published previously (e.g., Konnerup-Madsen, 2001) are unlikely to be explained by a major influx of low- δD meteoric fluids or by major degassing processes of either water or reducing fluids containing significant amounts of CH_4 and/or H_2 . Influence of assimilated organic matter rich sediments in the source region of the Ilímaussaq melts is one possible explanation (e.g., Sheppard, 1986a), but must have been very limited in volume so as not to affect the O- and Nd-isotopic compositions of late-stage amphiboles and cannot account for the isotopic composition of methane in the fluid inclusions (cf. Konnerup-Madsen et al., 1988; Konnerup-Madsen, 2001). Also, the existing differences in published amphibole-water fractionation factors that may be related either to the effects of pressure on hydrogen partitioning in the amphibole-water system and/or to the dependency of mineral-water fractionation on Fe in amphibole are unlikely to be large enough to account for the large range in measured δD values of the amphiboles. The favored process that may explain the low δD values for the amphiboles is secondary H-isotope exchange between internally generated, late-magmatic fluids and amphiboles, a process similar to that suggested for amphiboles from volcanic rocks by Miyagi and Matsubaya (2003). The mineralogy and fluid inclusion compositions of the Ilímaussaq rocks are compatible with an increase in the oxidation state of the magmatic system during late-stage cooling to the extent that earlier generated magmatic methane may be reoxidized. Comparison to data from other alkaline complexes indicates, that such a complex fluid evolution may not only be characteristic of the Ilímaussaq complex, but also of many other peralkaline igneous complexes worldwide. Detailed studies of the chemical (including $\text{Fe}^{3+}/\text{Fe}^{2+}$ ratios) and isotopic composition of late-stage hydrous minerals such as amphibole and biotite from a wide range of such complexes offer the best potential to test for the importance of such a complex fluid history to the evolution of alkaline to peralkaline rocks.

Acknowledgments—Laser ICP-MS measurements were carried out at the Large Scale Geochemical Facility supported by the European Community—Access to Research Infrastructure action of the Improving Human Potential Programme, contract HPRI-CT-1999-00008 awarded

to Prof. B. J. Wood (University of Bristol), which is gratefully acknowledged. Bruce Paterson provided invaluable help during these measurements. Elmar Reitter is thanked for his careful help during Nd isotope measurements, Gabi Stoschek for her help with the mass spectrometer and the oxygen and hydrogen isotope analyses. Constructive comments by E. Krogstad, B. Taylor, S. Sheppard and three anonymous reviewers helped to improve the quality of this work. We thank R. Ryerson for his editorial work. Thomas Wenzel helped to improve an earlier version of this manuscript. Financial support for this work was funded by the Deutsche Forschungsgemeinschaft (grant Ma-2135/1-2). This is contribution to the mineralogy of Ilímaussaq no. 118

Associate editor: F. J. Ryerson

REFERENCES

- Agemar T., Wörner G., and Heumann A. (1999) Stable isotopes and amphibole chemistry on hydrothermally altered granitoids in the North Chilean Precordillera: A limited role of meteoric water? *Contrib. Mineral. Petrol.* **136**, 331–344.
- Allaart J. H. (1969) The chronology and petrography of the Gardar dykes between Igaliko Fjord and Redekammen, South Greenland. *Rapp. Grønl. Geol. Under.* **25**, 26.
- Andersen T. (1997) Age and petrogenesis of the Qassarsuk carbonate-alkaline silicate volcanic complex in the Gardar rift, South Greenland. *Min. Mag.* **61**, 499–513.
- Armstrong J. T. (1991) Quantitative elemental analysis of individual microparticles with electron beam instruments. In *Electron Probe Quantitation* (eds. K. F. J. Heinrich and D. E. Newbury), pp. 261–315. Plenum.
- Ashwal L. D., Demaiffe D., and Torsvik T. H. (2002) Petrogenesis of neoproterozoic granitoids and related rocks from the Seychelles: The case for an Anedeian-type arc origin. *J. Petrol.* **43**, 45–83.
- Bailey J. C., Gwozdz R., Rose-Hansen J., and Sørensen H. (2001) Geochemical overview of the Ilímaussaq alkaline complex, South Greenland. *Geol. Greenl. Surv. Bull.* **190**, 35–53.
- Blaxland A. B., van Breeman O., and Steenfelt A. (1976) Age and origin of apatitic magmatism at Ilímaussaq, south Greenland: Rb-Sr study. *Lithos* **9**, 31–38.
- Botcher A. L. and O'Neil J. R. (1980) Stable isotope, chemical, and petrographic studies of high-pressure amphiboles and micas; evidence for metasomatism in the mantle source regions of alkali basalts and kimberlites. *Am. J. Sci.* **280A**, 594–621.
- Brandriss M. E., Nevle R. J., Bird D. K., and O'Neil J. R. (1995) Imprint of meteoric water on the stable isotope compositions of igneous and secondary minerals, Kap Edvard Holm complex, East Greenland. *Contrib. Mineral. Petrol.* **121**, 74–86.
- Chacko T., Cole D. R., and Horita J. (2001) Equilibrium oxygen, hydrogen and carbon isotope fractionation factors applicable to geologic systems. In *Stable Isotope Geochemistry* (eds. J. W. Valley and D. R. Cole), pp. 1–82. Reviews in Mineralogy 43. Min. Soc. Am.
- Chazot G., Lowry D., Menzies M., and Mathey D. P. (1997) Oxygen isotope composition of hydrous and anhydrous mantle peridotites. *Geochim. Cosmochim. Acta* **61**, 161–169.
- Clayton R. N. and Mayeda T. K. (1963) The use of bromine pentafluoride in the extraction of oxygen from oxides and silicates for isotope analysis. *Geochim. Cosmochim. Acta* **27**, 43–52.
- Cosca M. A., Essene E. J., and Bowman J. R. (1991) Complete chemical analyses of metamorphic hornblendes: Implications for normalizations, calculated H_2O activities and thermobarometry. *Contrib. Mineral. Petrol.* **108**, 472–484.
- Dahl-Jensen T., Thybo H., Hopper J., and Rosing M. (1998) Crustal structure at the SE Greenland margin from wide-angle and normal incidence seismic data. *Tectonophysics* **288**, 191–198.
- Dallai L., Ghezzi C., Sharp Z. D. (2003) Oxygen isotope evidence for crustal assimilation and magma mixing in the Granite Harbour intrusives, Northern Victoria Land, Antarctica. *Lithos* **67**, 135–151.
- Davies G. R. and Macdonald R. (1987) Crustal influences in the petrogenesis of the Naivasha basalt-comendite complex: Combined trace element and Sr-Nd-Pb isotope constraints. *J. Petrol.* **28**, 1009–1031.

- Déloué E., Albarède F., and Sheppard S. M. F. (1991) Hydrogen isotope heterogeneities in the mantle from ion-probe analysis of amphiboles from ultramafic rocks. *Earth Planet. Sci. Lett.* **105**, 543–553.
- Driesner T. (1997) The effect of pressure on deuterium-hydrogen fractionation in high-temperature water. *Science* **277**, 791–794.
- Eiler J. M. (2001) Oxygen isotope variations of basaltic lavas and upper mantle rocks. In *Stable Isotope Geochemistry* (eds. J. W. Valley and D. R. Cole), pp. 319–364. Reviews in Mineralogy 43. Min. Soc. Am.
- Emeleus C. H. and Upton B. G. J. (1976) The Gardar period in southern Greenland. In *Geology of Greenland* (eds. A. Escher and W. S. Watt), pp. 152–181. Geological Survey of Greenland.
- Engell J., Hansen J., Jensen M., Kunzendorf H., and Løvborg L. (1971) Beryllium mineralization in the Ilímaussaq Intrusion, South Greenland, with description of a field beryllometer and chemical methods. *Grøn. Geol. Unders.* **33**, 40 pp.
- Escher A. and Watt W. S. (1976) Geology of Greenland. Geological Survey of Greenland.
- Farver J. R. (1989) Oxygen self diffusion in diopside with application to cooling rate determinations. *Earth Planet. Sci. Lett.* **92**, 386–396.
- Farver J. R. and Giletti B. J. (1985) Oxygen diffusion in amphiboles. *Geochim. Cosmochim. Acta* **49**, 1403–1411.
- Feldstein S. N., Lange R. A., Vennemann T. W., and O'Neil J. R. (1996) Ferric-ferrous ratios, H₂O contents and D/H ratios of phlogopite and biotite from lavas of different tectonic regimes. *Contrib. Mineral. Petrol.* **126**, 51–66.
- Ferguson J. (1964) Geology of the Ilímaussaq alkaline intrusion, South Greenland. *Bull. Grøn. Geol. Under.* **39**, 82.
- Foland K. A., Landoll J. D., Henderson C. M. B., and Jiangfeng C. (1993) Formation of co-genetic quartz and nepheline syenites. *Geochim. Cosmochim. Acta* **57**, 697–704.
- Fowler J. M. B. and Harmon R. S. (1990) The oxygen isotope composition of lower crustal granulite xenoliths. In *Granulites and Crustal Evolution* (eds. D. Vielzeuf and P. Vidal), pp. 493–506. Kluwer.
- Garde A. A., Hamilton M. A., Chadwick B., Grocott J., and McCaffrey K. J. W. (2002) The Ketilidian orogen of South Greenland: Geochronology, tectonics, magmatism, and fore-arc accretion during Palaeoproterozoic oblique convergence. *Can. J. Earth Sci.* **39**, 765–793.
- Gérard O. and Jaoul O. (1989) Oxygen diffusion in San Carlos olivine. *J. Geophys. Res.* **94**, 4119–4128.
- Goldstein S. L., O'Nions R. K., and Hamilton P. J. (1984) A Sm-Nd isotopic study of the atmospheric dust and particulates from major river systems. *Earth Planet. Sci. Lett.* **70**, 221–236.
- Goodenough K. M., Upton B. G. J., and Ellam R. M. (2002) Long-term memory of subduction processes in the lithospheric mantle: Evidence from the geochemistry of basic dykes in the Gardar Province of south Greenland. *J. Geol. Soc. Lond.* **159**, 705–714.
- Graham C. M., Harmon R. S., and Sheppard S. M. F. (1984) Experimental hydrogen isotope studies: Hydrogen isotope exchange between amphibole and water. *Am. Mineral.* **69**, 128–138.
- Gregory R. T. Criss R. E. (1986) Stable isotopes in high temperature geological processes. In *Stable Isotopes* (eds. J. W. Valley, H. P. Taylor Jr., and J. R. O'Neil), pp. 91–128. Reviews in Mineralogy 16. Mineral. Soc. Am.
- Halama R., Marks, M., Brüggemann G. E., Siebel W., Wenzel T., and Markl G. (2004) Crustal contamination of mafic magmas: evidence from a petrological, geochemical and Sr-Nd-Os-O isotopic study of the Proterozoic Isortoq dike swarm, South Greenland. *Lithos* **74**, 199–232.
- Halama R., Waight T., and Markl G. (2002) Geochemical and isotopic zoning patterns of plagioclase megacrysts in gabbroic dykes from the Gardar Province, South Greenland: Implications for crystallisation processes in anorthositic magmas. *Contrib. Mineral. Petrol.* **144**, 109–127.
- Halama R., Wenzel T., Upton B. G. J., Siebel W., and Markl G. (2003) A geochemical and Sr-Nd-O isotopic study of the Proterozoic Eriksfjord Basalts, Gardar Province, South Greenland. Reconstruction of OIB-signature in crustally contaminated rift-related basalts. *Min. Mag.* **67**, 831–854.
- Harris C. (1995) Oxygen isotope geochemistry of the Mesozoic anorthogenic complexes of Damaraland, northwest Namibia: Evidence for crustal contamination and its effects on silica saturation. *Contrib. Mineral. Petrol.* **122**, 308–321.
- Harris C., Whittingham A. M., Milner S. C., and Armstrong R. A. (1990) Oxygen isotope geochemistry of the silicic volcanic rocks of the Etendeka/Parana Province: Source constraints. *Geology* **18**, 1119–1121.
- Harris C., Marsh J. S., and Milner S. C. (1999) Petrology of the alkaline core of the Messum igneous complex, Namibia: Evidence for the progressively decreasing effect of crustal contamination. *J. Petrol.* **40**, 1377–1397.
- Harris C. and Ashwal L. D. (2002) The origin of low $\delta^{18}\text{O}$ granites and related rocks from the Seychelles. *Contrib. Mineral. Petrol.* **143**, 366–376.
- Heaman L. M. and Machado N. (1992) Timing and origin of midcontinent rift alkaline magmatism, North America: Evidence from the Coldwell Complex. *Contrib. Mineral. Petrol.* **110**, 289–303.
- Hoefs J. (1997) Stable Isotope Geochemistry. Springer.
- Horibe Y. and Craig H. (1995) D/H fractionation in the system methane-hydrogen-water. *Geochim. Cosmochim. Acta* **59**, 5209–5217.
- Horita J., Driesner T., and Cole D. R. (1999) Pressure effect on hydrogen isotope fractionation between brucite and water at elevated temperatures. *Science* **286**, 1545–1547.
- Jacobson S. B. and Wasserburg G. J. (1980) Sm-Nd isotopic evolution of chondrites. *Earth Planet. Sci. Lett.* **50**, 139–155.
- Kalsbeek F. and Taylor P. N. (1985) Isotopic and chemical variation in granites across a Proterozoic continental margin—the Ketilidian mobile belt of South Greenland. *Earth Planet. Sci. Lett.* **73**, 65–80.
- Kogarko L. N., Kosztolanyi Ch., and Raybchikov I. D. (1987) Geochemistry of the reduced fluid in alkali magmas. *Geochem. Int.* **24**, 20–27.
- Konnerup-Madsen J. (1980) Fluid inclusions in minerals from igneous rocks belonging to Precambrian continental Gardar rift province, south Greenland: The alkaline Ilímaussaq intrusion and the alkali acidic igneous complexes. Ph.D. thesis, Copenhagen University.
- Konnerup-Madsen J. (2001) A review of the composition and evolution of hydrocarbon gases during solidification of the Ilímaussaq alkaline complex, South Greenland. *Geol. Greenl. Surv. Bull.* **190**, 159–166.
- Konnerup-Madsen J., Larsen E., and Rose-Hansen J. (1979) Hydrocarbon-rich fluid inclusions in minerals from the alkaline Ilímaussaq intrusion, South Greenland. *Bull. Mineral.* **102**, 642–653.
- Konnerup-Madsen J. and Rose-Hansen J. (1984) Composition and significance of fluid inclusions in the Ilímaussaq peralkaline granite, South Greenland. *Bull. Mineral.* **107**, 317–326.
- Konnerup-Madsen J., Kreulen R., and Rose-Hansen J. (1988) Stable isotope characteristics of hydrocarbon gases in the alkaline Ilímaussaq complex, South Greenland. *Bull. Mineral.* **111**, 567–576.
- Kramm U. and Kogarko L. N. (1994) Nd and Sr isotope signatures of the Khibina and Lovozero apatitic centres, Kola Province, Russia. *Lithos* **32**, 225–242.
- Kyser T. K. (1986) Stable isotope variations in the mantle. In *Stable Isotopes* (eds. J. W. Valley, H. P. Taylor Jr., and J. R. O'Neil), pp. 141–162. Reviews in Mineralogy 16. Mineral. Soc. Am.
- Larsen L. M. (1976) Clinopyroxenes and coexisting mafic minerals from the alkaline Ilímaussaq intrusion, south Greenland. *J. Petrol.* **17**, 258–290.
- Larsen L. M. (1977) Aenigmatites from the Ilímaussaq intrusion, south Greenland: Chemistry and petrological implications. *Lithos* **10**, 257–270.
- Larsen L. M. (1981) Chemistry of feldspars in the Ilímaussaq augite syenite with additional data on some other minerals. *Rapp. Grøn. Geol. Under.* **103**, 31–37.
- Larsen L. M. and Steenfelt A. (1974) Alkali loss and retention in an iron-rich peralkaline phonolite dyke from the Gardar province, south Greenland. *Lithos* **7**, 81–90.
- Larsen L. M. and Sørensen H. (1987) The Ilímaussaq intrusion-progressive crystallization and formation of layering in an apatitic magma. In *Alkaline Igneous Rocks* (eds. J. G. Fitton and B. G. J. Upton), pp. 473–488. Special Publication 30. Geol. Soc.
- Liew T. C. and Hofmann A. W. (1988) Precambrian crustal components, plutonic associations, plate environment of the Hercynian Fold Belt of central Europe: Indications from a Nd and Sr isotopic study. *Contrib. Mineral. Petrol.* **98**, 129–138.

- Lugmair G. W. and Marti K. (1978) Lunar initial $^{143}\text{Nd}/^{144}\text{Nd}$: Differential evolution of the lunar crust and mantle. *Earth Planet. Sci. Lett.* **39**, 349–357.
- Lutz T. M., Foland K. A., Faul H., and Srogi L. A. (1988) The strontium and oxygen isotopic record of hydrothermal alteration of syenites from the Abu Khruq complex, Egypt. *Contrib. Mineral. Petrol.* **98**, 212–223.
- Markl G. (2001a) Stability of Na-Be minerals in late-magmatic fluids of the Ilímaussaq alkaline complex, South Greenland. *Geol. Greenl. Surv. Bull.* **190**, 145–158.
- Markl G. (2001b) A new type of silicate liquid immiscibility in peralkaline nepheline syenites (lujavrites) of the Ilímaussaq complex, South Greenland. *Contrib. Mineral. Petrol.* **141**, 458–472.
- Markl G., Marks M., Schwinn G., and Sommer H. (2001a) Phase equilibrium constraints on intensive crystallization parameters of the Ilímaussaq Complex, South Greenland. *J. Petrol.* **42**, 2231–2258.
- Markl G., Marks M., and Wirth R. (2001b) The influence of T, aSiO_2 , $f\text{O}_2$ on exsolution textures in Fe-Mg olivine: An example from augite syenite of the Ilímaussaq Intrusion, South Greenland. *Am. Mineral.* **86**, 36–46.
- Marks M. and Markl G. (2001) Fractionation and assimilation processes in the alkaline augite syenite unit of the Ilímaussaq Intrusion, South Greenland, as deduced from phase equilibria. *J. Petrol.* **42**, 1947–1969.
- Marks M. and Markl G. (2003) Ilímaussaq “en miniature:” Closed-system fractionation in an apatitic dyke rock from the Gardar province, south Greenland. *Min. Mag.* **67**, 893–919.
- Marks M., Vennemann T. W., Siebel W., and Markl G. (2003) Quantification of magmatic and hydrothermal processes in a peralkaline syenite-alkali granite complex based on textures, phase equilibria, and stable and radiogenic isotopes. *J. Petrol.* **44**, 1247–1280.
- Mathez E. A. (1984) Influence of degassing on oxidation states of basaltic magmas. *Nature* **310**, 371–375.
- Matvey D., Lowry D., and Macpherson C. (1994) Oxygen isotope composition of mantle peridotite. *Earth Planet. Sci. Lett.* **128**, 231–241.
- Mingram B., Trumbull R. B., Littman S., and Gerstenberger H. (2000) A petrogenetic study of anorogenic felsic magmatism in the Cretaceous Paresis ring complex, Namibia: Evidence for mixing of crust and mantle-derived components. *Lithos* **54**, 1–22.
- Mitchell R. H. (1990) A review of the compositional variation of amphiboles in alkaline plutonic complexes. *Lithos* **26**, 135–156.
- Miyagi I., Matsubaya O., and Nakashima S. (1998) Change in D/H ratio, water content and color during dehydration of hornblende. *Geochem. J.* **32**, 33–48.
- Miyagi I. and Matsubaya O. (2003) Hydrogen isotopic composition of hornblende and biotite phenocrysts from Japanese island arc volcanoes: Evaluation of alteration process of the hydrogen isotopic ratios by degassing and re-equilibration. *J. Volc. Geoth. Res.* **126**, 157–168.
- Nabelek P. L., O’Neil J. R., and Papike J. J. (1983) Vapour phase exsolution as the controlling factor in hydrogen isotope variation in granitic rocks; the Notche Peak granitic stock, Utah. *Earth Planet. Sci. Lett.* **66**, 137–150.
- Nevle R. J., Brandriss M. E., Bird D. K., MacWilliams M. O., and O’Neil J. R. (1994) Tertiary plutons monitor climate change in East Greenland. *Geology* **22**, 775–778.
- Nicholson S. W. and Shirey S. B. (1990) Midcontinent Rift Volcanism in the Lake Superior Region: Sr, Nd, and Pb isotopic evidence for a mantle plume origin. *J. Geophys. Res.* **95**, 10851–10868.
- Nielsen B. L. and Steenfelt A. (1979) Intrusive events at Kvanefjeld in the Ilímaussaq igneous complex. *Bull. Geol. Soc. Denmark* **27**, 143–155.
- Nivin V. A., Devirts A. L., and Lagutina Y. P. (1995) The origin of the gas phase in the Lovozero massif based on hydrogen-isotope data. *Geochem. Int.* **32**, 65–71.
- O’Neil J. R. (1986) Stable isotopes in high temperature geological processes. In *Stable Isotopes* (eds. J. W. Valley, H. P. Taylor Jr., and J. R. O’Neil), pp. 1–40. Reviews in Mineralogy 16. Mineral. Soc. Am.
- Paslick C. R., Halliday A. N., Davies G. R., Mezger K., and Upton B. G. J. (1993) Timing of proterozoic magmatism in the Gardar Province, southern Greenland. *Bull. Geol. Soc. Am.* **105**, 272–278.
- Perry F. V., Baldrige W. S., and DePaolo D. J. (1987) Role of asthenosphere and lithosphere in the genesis of late cenozoic basaltic rocks from the Rio Grande rift and adjacent regions of the Southwestern United States. *J. Geophys. Res.* **92**, 9193–9213.
- Petersilie I. A. and Sørensen H. (1970) Hydrocarbon gases and bituminous substances in rocks from the Ilímaussaq alkaline intrusion, South Greenland. *Lithos* **3**, 59–76.
- Potter J. (2002) Textural and compositional evidence for the origin of hydrocarbons in alkaline igneous rocks. *Beih. Eur. J. Mineral.* **14**, 132.
- Potter J., Rankin A. H., Treloar P. J., Nivin V. A., Ting W., and Ni P. (1998) A preliminary study of methane inclusions in alkaline igneous rocks of the Kola igneous province, Russia: Implications for the origin of methane in igneous rocks. *Eur. J. Mineral.* **10**, 1167–1180.
- Poulsen V. (1964) The sandstones of the Precambrian Eriksfjord Formation in South Greenland. *Rapp. Grønl. Geol. Under.* **2**, 16.
- Pushkar P., McBirney A. R., and Kudo A. M. (1972) The isotopic composition of strontium in Central American ignimbrites. *Bull. Volcanol.* **35**, 265–294.
- Ranløv J. and Dymek R. F. (1991) Compositional zoning in hydrothermal aegirine from fenites in the Proterozoic Gardar Province, South Greenland. *Eur. J. Mineral.* **3**, 837–853.
- Richet P., Bottinga Y., and Javoy M. (1977) A review of hydrogen, carbon, nitrogen, oxygen, sulphur, and chlorine stable isotope fractionation among gaseous molecules. *Annu. Rev. Earth Planet. Sci.* **5**, 65–110.
- Roddick J. C., Sullivan R. W., and Dudas F. Ö. (1992) Precise calibration of Nd tracer isotopic composition for Sm-Nd studies. *Chem. Geol.* **97**, 1–8.
- Rose-Hansen J. and Sørensen H. (2001) Minor intrusions of peralkaline microsyenite in the Ilímaussaq alkaline complex, South Greenland. *Bull. Geol. Soc. Denmark* **48**, 9–29.
- Rumble D. and Hoering T. C. (1994) Analysis of oxygen and sulfur isotope ratios in oxide and sulfide minerals by spot heating with a carbon dioxide laser in a fluorine atmosphere. *Acc. Chem. Res.* **27**, 237–241.
- Salvi S. and Williams-Jones A. E. (1997) Fischer-Tropsch synthesis of hydrocarbons during sub-solidus alteration of the Strange Lake peralkaline granite, Quebec/Labrador, Canada. *Geochim. Cosmochim. Acta* **61**, 83–99.
- Sato M. (1978) Oxygen fugacity of basaltic magmas and the role of gas-forming elements. *Geophys. Res. Lett.* **5**, 447–449.
- Schmitt A. K., Emmermann R., Trumbull R. B., Bühn B., and Henjes-Kunst F. (2000) Petrogenesis and $^{40}\text{Ar}/^{39}\text{Ar}$ Geochronology of the Brandberg Complex, Namibia: Evidence for a major mantle contribution in metaluminous and peralkaline granites. *J. Petrol.* **41**, 1207–1239.
- Sharp Z. D. (1990) A laser-based microanalytical method for the in-situ determination of oxygen isotope ratios of silicates and oxides. *Geochim. Cosmochim. Acta* **54**, 1353–1357.
- Sharp Z. D., Atudorei V., and Durakiewicz T. (2001) A rapid method for determining the hydrogen and oxygen isotope ratios from water and solid hydrous substances. *Chem. Geol.* **178**, 197–210.
- Sheppard S. M. F. (1986a) Igneous rocks: III. Isotopic case studies of magmatism in Africa, Eurasia. In *Stable Isotopes* (eds. J. W. Valley, H. P. Taylor Jr., and J. R. O’Neil), pp. 319–368. Reviews in Mineralogy 16. Mineral. Soc. Am.
- Sheppard S. M. F. (1986b) Characterization and isotopic variations in natural waters. In *Stable Isotopes* (eds. J. W. Valley, H. P. Taylor Jr., and J. R. O’Neil), pp. 165–181. Reviews in Mineralogy 16. Mineral. Soc. Am.
- Sørensen H. (2001) Brief introduction to the Geology of the Ilímaussaq alkaline complex, South Greenland. *Geol. Greenl. Surv. Bull.* **190**, 7–24.
- Sørensen H., Rose-Hansen J., Nielsen B. L., Løvborg L., Sørensen E., and Lundgaard T. (1974) The uranium deposit at Kvanefjeld, the Ilímaussaq intrusion, South Greenland. *Grønl. Geol. Unders.* **60**, 54 pp.
- Späth A., Le Roex A. P., and Opiyo-Akech N. (2001) Plume-lithosphere interaction and the origin of continental rift-related alkaline volcanism—the Chyulu hills volcanic province, Southern Kenya. *J. Petrol.* **42**, 765–787.

- Stevenson R., Upton B. G. J., and Steenfelt A. (1997) Crust-mantle interaction in the evolution of the Ilímaussaq Complex, South Greenland: Nd isotopic studies. *Lithos* **40**, 189–202.
- Suzuoki T. and Epstein S. (1976) Hydrogen isotope fractionation between OH-bearing minerals and water. *Geochim. Cosmochim. Acta* **40**, 1229–1240.
- Taylor H. P. (1974) The application of oxygen and hydrogen isotope studies to problems of hydrothermal alteration and ore deposition. *Econ. Geol.* **69**, 843–883.
- Taylor B. E. (1986) Stable isotopes in high temperature geological processes. In *Stable Isotopes* (eds. J. W. Valley, H. P. Taylor Jr., and J. R. O'Neil), pp. 185–226. Reviews in Mineralogy 16. Mineral. Soc. Am.
- Taylor B. E., Eichelberger J. C., and Westrich H. R. (1983) Hydrogen isotopic evidence of rhyolitic magma degassing during shallow intrusion and eruption. *Nature* **306**, 541–545.
- Taylor P. N., Jones N. W., and Moorbath S. (1984) Isotopic assessment of relative contributions from crust and mantle sources to the magma genesis of Precambrian granitoid rocks. *Phil. Trans. R. Soc. Lond. A* **310**, 605–625.
- Taylor H. P. Jr. and Sheppard S. M. F. (1986) Stable isotopes in high temperature geological processes. In *Stable Isotopes* (eds. J. W. Valley, H. P. Taylor Jr., and J. R. O'Neil), pp. 227–269. Reviews in Mineralogy 16. Mineral. Soc. Am.
- Upton B. G. J. (1987) Gardar mantle xenoliths: Igdlutalik, South Greenland. *Rapp. Grøn. Geol. Under.* **150**, 37–43.
- Upton B. G. J. Emeleus C. H. (1987) Mid-Proterozoic alkaline magmatism in southern Greenland: The Gardar province. In *The Alkaline Rocks*, Vol. 30 (eds. J. G. Fitton and B. G. J. Upton), 449–471. Blackwell Scientific.
- Upton B. G. J., Emeleus C. H., Heaman L. M., Goodenough K. M., and Finch A. (2003) Magmatism of the mid-Proterozoic Gardar Province, South Greenland: Chronology, petrogenesis and geological setting. *Lithos* **68**, 43–65.
- Valley J. W., Kitchen N., Kohn M. J., Niendorf C. R., and Spicuzza M. J. (1995) UWG-2, a garnet standard for oxygen isotope ratios: Strategies for high precision and accuracy with laser heating. *Geochim. Cosmochim. Acta* **59**, 5223–5231.
- Vennemann T. W. and O'Neil J. R. (1993) A simple and inexpensive method of hydrogen isotope and water analyses of minerals and rocks based on zinc reagent. *Chem. Geol.* **103**, 227–234.
- Vennemann T. W. and O'Neil J. R. (1996) Hydrogen isotope exchange reactions between hydrous minerals and molecular hydrogen: I. A new approach for the determination of hydrogen isotope fractionation at moderate temperatures. *Geochim. Cosmochim. Acta* **60**, 2437–2451.
- Waight T., Baker J., and Willigers B. (2002) Rb isotope dilution analyses by MC-ICPMS using Zr to correct for mass fractionation: Towards improved Rb-Sr geochronology? *Chem. Geol.* **186**, 99–116.
- Zheng Y.-F. (1993) Calculation of oxygen isotope fractionation in hydroxyl-bearing silicates. *Earth Planet. Sci. Lett.* **120**, 247–263.
- Zindler A. and Hart S. R. (1986) Chemical geodynamics. *Annu. Rev. Earth Planet. Sci.* **14**, 493–571.